

New Estimation Approaches for the Linear Ballistic Accumulator Model

David Gunawan^{1,2}, Scott Brown³, Robert Kohn^{1,2}, and Minh-Ngoc Tran^{2,4*}

November 2, 2021

Abstract

The Linear Ballistic Accumulator (LBA) model of Brown and Heathcote (2008) is used as a measurement tool to answer questions about applied psychology. These analyses involve parameter estimation and model selection, and modern approaches use hierarchical Bayesian methods and Markov chain Monte Carlo (MCMC) to estimate the posterior distribution of the parameters. Although there are a range of approaches used for model selection, they are all based on the posterior samples produced via MCMC, which means that the model selection inferences inherit properties of the MCMC sampler. We address these constraints by proposing two new approaches to the Bayesian estimation of the hierarchical LBA model. Both methods are qualitatively different from all existing approaches, and are based on recent advances in particle-based Monte-Carlo methods. The first approach is based on particle MCMC, using Metropolis-within-Gibbs steps and the second approach uses a version of annealed importance sampling. Both methods have important differences from all existing methods, including greatly improved sampling efficiency and parallelisability for high-performance computing. An important further advantage of our annealed importance sampling algorithm is that an estimate of the marginal likelihood is obtained as a byproduct of sampling. This makes it straightforward to then apply model selection via Bayes factors. The new approaches we develop provide opportunities to apply the LBA model with greater confidence than before, and to extend its use to previously intractable cases. We illustrate the proposed methods with pseudo-code, and by application to simulated and real datasets.

* ¹:School of Economics, UNSW Business School, University of New South Wales. ²:ARC Centre of Excellence for Mathematical and Statistical Frontiers (ACEMS). ³:School of Psychology, University of Newcastle ⁴:Discipline of Business Analytics, University of Sydney.

Keywords: Adaptive estimation; Annealed Importance Sampling; Hierarchical model; Marginal likelihood; Particle Metropolis within Gibbs.

1 Introduction

The Linear Ballistic Accumulator (LBA) model provides a tractable model of decision making. The LBA model is simpler than some other models of choice response time because it eliminates complexities such as competition between alternatives (Ratcliff, 1978; Ratcliff and Rouder, 1998; Brown and Heathcote, 2005), and passive decay of evidence (Ratcliff and Smith, 2004; Usher and McClelland, 2001). The simplicity of the model allows analytic solutions for choices between any number of alternatives. Like other evidence accumulation models, the LBA has been used to address important theoretical and applied questions about human cognition, both in the general population and in clinical groups (for reviews, see e.g., Ratcliff et al., 2016; Donkin and Brown, 2018).

When used in this way, as a psychometric tool, key inferences are drawn from parameter estimates and from comparisons between different versions of the LBA fit to the same data. These comparisons rely on accurate parameter estimation and valid model selection procedures, but these can be difficult problems. Most modern applications of the model use hierarchical structures estimated in a Bayesian framework. The posterior distributions over the parameters are most often estimated using Markov chain Monte Carlo (MCMC), with proposals drawn by differential evolution MCMC (DE-MCMC: Turner et al., 2013). This procedure alleviates some of the challenging aspects of parameter estimation in the LBA, caused by the substantial correlations between model parameters. Inferences about model selection are almost always carried out by estimating a marginal likelihood, or some quantity that behaves approximately like the marginal likelihood, from the MCMC samples. Commonly used model selection metrics include the deviance information criterion (DIC: Spiegelhalter et al., 2014) and the Watanabe (or “widely applicable”) information criterion (WAIC: Watanabe, 2010). Very recent developments have investigated ways to approximate the marginal likelihood more directly, either by bridge sampling (Gronau et al., 2017), or by brute force sampling from the prior (Evans and Brown, 2018). These approaches are particularly promising, because they have the potential to support model selection via Bayes factors. However, these approaches have not yet become standard, or widely adopted. The brute force approach of Evans and Brown requires specialized computing hardware (a general purpose graphical processing unit) to be computationally feasible, and the method’s extension to hierarchical models with random effects is not quite fully developed. On the other

hand, the bridge sampling approach of Gronau et al. (2017) is promising even for random effects models, and has low computational overheads. However – and like all the other methods reviewed above, except for the brute force approach – the bridge sampling method has as its starting point posterior samples generated by DE-MCMC. This common feature of all the model selection approaches has the potential to cause weaknesses in statistical inference. In cases where the DE-MCMC samples provide an imperfect representation of the posterior, for whatever reason, the different model selection methods will be wrong. Even worse, they are all quite likely to agree with each other on the wrong inference, because they are all based on the same samples. While the DE-MCMC sampler appears to work well in practice, it also suffers from the usual problems associated with random walk samplers in high dimensional problems, including high autocorrelation between samples, and slow or uncertain convergence in some problems.

We propose two new methods for estimating the model. Both methods provide new ways of drawing posterior samples, without using DE-MCMC. The methods produce samples efficiently. The first of our two approaches is based on the particle Metropolis within Gibbs (PMwG) method of Gunawan et al. (2017). The basic idea of the PMwG method is to define an appropriate target distribution on an augmented space that includes the standard model parameters as well as multiple copies of the individual random effects (“particles”). Gunawan et al. (2017) showed that the augmented target density of the PMwG algorithm has as its marginal density the joint posterior density of the parameters and individual random effects. The PMwG algorithm that we propose represents an important new alternative to the standard DE-MCMC approach which has been used for LBA estimation since Turner et al. (2013). Like DE-MCMC, PMwG uses Markov Chains to draw samples, which can then be used to address model selection or parameter estimation questions in the standard ways. In our investigations, the PMwG method produces samples with greater efficiency and much lower autocorrelation than DE-MCMC. Nevertheless, the PMwG method has similar in-principle drawbacks as all MCMC methods: it is difficult to determine whether the generated Markov chain has converged to draws from the posterior and it is also difficult to obtain an estimate of the marginal likelihood. We note, however, that the PMwG approach is also an important building block of our second approach.

As an alternative to all MCMC approaches, including DE-MCMC and our PMwG sampler, our second approach is based on the annealed importance sampling (AIS) approach (Neal, 2001). This is an importance sampling method in which samples are first drawn from an easily-generated distribution and then moved towards the posterior distribution of interest. Our proposed annealing approach builds on the

work by Duan and Fulop (2015), Neal (2001), and Del Moral et al. (2006). We call our algorithm Annealed Importance Sampling with Intractable Likelihood for random effects models (AISIL-RE). Our approach has three main steps when transitioning from one intermediate density to another: reweighting, resampling, and Markov moves. Moving from one intermediate target density to the next target density is accomplished via reweighting the particles. As the algorithm proceeds, the variability of the importance weights increases leading to sample impoverishment. One way to avoid this problem is to resample the particles proportionally to their normalised weights (e.g., Del Moral et al., 2006). However, repeated reweighting and resampling can lead to particle depletion (Duan and Fulop, 2015). To avoid this, we use Markov moves based on our new PMwG sampler, that leaves the annealed target density invariant, but which boost the diversity of the particles such that they are better approximations to the annealed target density, at each intermediate density of the annealing process. The AISIL-RE algorithm is also related to the annealed importance sampling scheme developed in Gunawan et al. (2018), but their method is applied to time series state space models and their particle Gibbs sampler and the Markov move steps in the annealing are very different to the approach taken in the present article.

The AISIL-RE approach has some advantages over the PMwG approach, and over all MCMC approaches in general. Most importantly, AISIL-RE bypasses some of the difficult problems of assessing convergence and autocorrelation in Markov chain samplers such as DE-MCMC and PMwG. The AISIL-RE method is also easily parallelized, across the annealed samples, which is an important consideration for high-performance computing. This opens the possibility of applying the sampler to much larger-scale problems than have previously been tractable for the LBA, and for evidence accumulation modelling in general. Finally, AISIL-RE provides a direct estimate of the model’s marginal likelihood, during computation which makes model selection via Bayes factor straightforward to implement.

2 The Linear Ballistic Accumulator (LBA) Model

We first consider a special case without individual differences, so that a single set of parameters describes the behaviour of all responses in the data. The i th single observation in a typical choice experiment will contain two pieces of information. The first information is the response choice, which we denote $RE_i \in \{1, \dots, C\}$, where C is the number of response alternatives. The second piece is the response time (RT),

which we denote $RT_i \in (0, \infty)$.

The LBA model represents a choice between C alternatives ($C = 2, 3, \dots$) using C different evidence accumulators, one for each response. It assumes that evidence accumulates for each of the C alternatives at the beginning of a decision trial. Each accumulator begins with an independent amount of starting evidence k_c which is sampled independently for each accumulator from a continuous uniform distribution $k_c \sim U(0, A)$. The evidence for accumulator c increases at a rate d_c (the drift rate for the c th response alternative) which is sampled independently for each accumulator from a normal distribution with mean v^c and standard deviation s , so $d_c \sim N(v^c, s)$, although other non-normal distributions are possible (Terry et al., 2015). To satisfy the scaling conditions of the model, it is common to set the variance of the sampled drift rates to one, $s = 1$ (but see also: Donkin et al., 2009). Each accumulator gathers evidence until one accumulator reaches a response threshold b . The LBA model assumes that the observed RT is the sum of the decision time, plus some extra time τ for the non-decision process such as motor execution and stimulus encoding. For simplicity τ is usually assumed to be constant across trials. Thus, the final observed RT is given by

$$RT = \min_c \left(\frac{b - k_c}{d_c} \right) + \tau.$$

Let $T_c = (b - k_c)/d_c + \tau$ be the time for accumulator c to reach the threshold b . Brown and Heathcote (2008) derive the cdf and pdf of T_c as

$$\begin{aligned} F_c(t) = & 1 + \frac{b - A - (t - \tau)v^c}{A} \Phi \left(\frac{b - A - (t - \tau)v^c}{(t - \tau)s} \right) - \frac{b - (t - \tau)v^c}{A} \Phi \left(\frac{b - (t - \tau)v^c}{(t - \tau)s} \right) \\ & + \frac{(t - \tau)s}{A} \phi \left(\frac{b - A - (t - \tau)v^c}{(t - \tau)s} \right) - \frac{(t - \tau)s}{A} \phi \left(\frac{b - (t - \tau)v^c}{(t - \tau)s} \right) \\ f_c(t) = & \frac{1}{A} \left[-v^c \Phi \left(\frac{b - A - (t - \tau)v^c}{(t - \tau)s} \right) + s \phi \left(\frac{b - A - (t - \tau)v^c}{(t - \tau)s} \right) \right. \\ & \left. + v^c \Phi \left(\frac{b - (t - \tau)v^c}{(t - \tau)s} \right) - s \phi \left(\frac{b - (t - \tau)v^c}{(t - \tau)s} \right) \right]. \end{aligned} \quad (1)$$

If the observed response choice is $RE = c$ and $RT \in (t, t + d\delta t)$, then

$$P(RE = c, RT \in t + \delta t) = P(T_c \in t + \delta t, T_k > t, k \neq c) = f_c(t)\delta t \times \prod_{k \neq c} (1 - F_k(t)).$$

Hence, the joint density of $RT = t$ and $RE = c$ is

$$\text{LBA}(c, t | b, A, v, s, \tau) = f_c(t) \times \prod_{k \neq c} (1 - F_k(t)),$$

with respect to the product measure $dt\mu(dc)$ where dt is Lebesgue measure and $\mu(\cdot)$ is the counting measure on the integers $1, \dots, C$.

Assuming independent decisions for a vector of N responses RE with corresponding response times RT , the likelihood function is given by

$$p(RE, RT|b, A, v, s, \tau) = \prod_{i=1}^N \text{LBA}(RE_i, RT_i|b, A, v, s, \tau).$$

2.1 Hierarchical Bayesian Implementation of the Linear Ballistic Accumulator (LBA) Model

Our model setup for the hierarchical LBA model in this section is motivated by the data first presented by Forstmann et al. (2008), collected from the decisions of 19 young subjects. The participants were asked to decide, repeatedly, whether a cloud of semi-randomly moving dots appeared to move to the left or to the right. Before each decision trial, subjects were instructed about what quality of their decision-making they should emphasise. For some trials, they were asked to respond as accurately as possible, for other trials they were asked to respond at their own pace, and for other trials they were asked to respond as quickly as possible. We label these conditions, in order: “accuracy emphasis” (condition 1); “neutral emphasis” (condition 2); and “speed emphasis” (condition 3). The different conditions were randomly mixed from trial to trial, with the subjects cued by a word which appeared on screen before each decision stimulus. Each subject made 280 decisions in each condition (840 trials in total). See Forstmann et al. (2008) for greater details on the procedure, and the data, including the associated neuroimaging measurements, which are not considered here.

To model the differences between the three conditions in the experiment, we follow Forstmann et al. (2008) and define a vector of response threshold parameters $\mathbf{b} = (b^{(1)}, b^{(2)}, b^{(3)})$, so that $b^{(1)}$, $b^{(2)}$, and $b^{(3)}$ are used for accuracy, neutral, and speed conditions respectively. $RE_{i,j}$ and $RT_{i,j}$ denote the i th response from the j th subject. Also following Forstmann et al., we collapse data across right-moving and left-moving stimuli, and so we index means of the drift rate distributions as $v = \{v^{(1)}, v^{(2)}\}$, where $v^{(1)}$ is the drift rate for the accumulator corresponding to incorrect response and $v^{(2)}$ is the drift rate for the accumulator corresponding to the correct response choice. We assume that the standard deviation of the drift rate distribution is always $s = 1$. Together, these assumptions imply that each subject $j, j = \{1, \dots, S\}$, has the vector of random effects,

$$(b_j^{(1)}, b_j^{(2)}, b_j^{(3)}, A_j, \tau_j, v_j^{(1)}, v_j^{(2)}).$$

Let Z be the number of conditions in the experiment, $Z = 3$ here. With the usual assumptions of independence, the conditional density of all the observations is

$$p(RT, RE | \mathbf{b}, \mathbf{A}, \boldsymbol{\tau}, \mathbf{v}) = \prod_{j=1}^S \prod_{i=1}^N \prod_{z=1}^Z \text{LBA} \left(RE_{i,j,z}, RT_{i,j,z} | b_j^{(z)}, A_j, v_j^{(1)}, v_j^{(2)}, \tau_j \right). \quad (2)$$

Each of the individual random effects is restricted to be positive. Respecting this, Turner et al. (2013) specified an independent truncated normal distribution for the individual random effects parameters, and this has become standard in hierarchical applications of the LBA since then. Turner et al. (2013) also found, as have others, that the posterior distributions of the individual random effects are highly correlated. Despite this, standard practice has been to specify independent distributions for each of them.

To improve both the computational efficiency of our algorithms and the precision of inference, we abandon both of these standard assumptions about hierarchical structure. This is explained more fully in the last paragraph of this section. Instead, we adopt the hierarchical model based on multivariate normal distributions of log-transformed random effects, with explicitly-estimated covariance structures: For each subject $j = 1, \dots, S$, we define the vector of random effects,

$$\boldsymbol{\alpha}_j = \left(\alpha_{b_j^{(1)}}, \alpha_{b_j^{(2)}}, \alpha_{b_j^{(3)}}, \alpha_{A_j}, \alpha_{v_j^{(1)}}, \alpha_{v_j^{(2)}}, \alpha_{\tau_j} \right), \quad \text{where} \\ \alpha_{b_j^{(z)}} = \log \left(b_j^{(z)} \right), \alpha_{A_j} = \log \left(A_j \right), \alpha_{v_j^{(c)}} = \log \left(v_j^{(c)} \right), \alpha_{\tau_j} = \log \left(\tau_j \right); j = 1, \dots, S. \quad (3)$$

Let $D_\alpha = 7$ be the dimension of $\boldsymbol{\alpha}_j$. The prior distribution of the vector $\boldsymbol{\alpha}_j$ is modeled as

$$\boldsymbol{\alpha}_j | \boldsymbol{\mu}_\alpha, \boldsymbol{\Sigma}_\alpha \sim N(\boldsymbol{\mu}_\alpha, \boldsymbol{\Sigma}_\alpha). \quad (4)$$

We take the prior for $\boldsymbol{\mu}_\alpha$ as

$$\boldsymbol{\mu}_\alpha \sim N(0, I_{D_\alpha}), \quad (5)$$

which is non-informative as we argue below. We take the marginally non-informative prior of Huang and Wand (2013) for $\boldsymbol{\Sigma}_\alpha$:

$$\boldsymbol{\Sigma}_\alpha | a_1, \dots, a_{D_\alpha} \sim IW(v_\alpha + D_\alpha - 1, 2v_\alpha \text{diag}(1/a_1, \dots, 1/a_{D_\alpha})), \\ a_1, \dots, a_{D_\alpha} \sim IG\left(\frac{1}{2}, \frac{1}{\mathcal{A}_d^2}\right), d = 1, \dots, D_\alpha \quad (6)$$

where $v_\alpha, \mathcal{A}_1, \dots, \mathcal{A}_{D_\alpha}$ are positive scalars and $\text{diag}(1/a_1, \dots, 1/a_{D_\alpha})$ is a diagonal matrix with diagonal elements $1/a_1, \dots, 1/a_{D_\alpha}$. The notation $IW(a, A)$ means an inverse Wishart distribution with degrees of freedom a and scale matrix A and the notation

$IG(a, b)$ means an inverse Gamma distribution with scale parameter a and shape parameter b . Huang and Wand show that Eq. (6) induces half-t(v_α, \mathcal{A}_d) distributions for each standard deviation term in Σ_α and setting $v_\alpha = 2$ leads to marginally uniform distributions for all the correlation terms in Σ_α . In our application, we set $v_\alpha = 2$ and $\mathcal{A}_d = 1$ for all $d = 1, \dots, D_\alpha$. These prior densities cover most possible values in practice, and are diffuse. The specification we have used implies that the prior for the random effects vector $\exp(\alpha_j)|\mu_\alpha, \Sigma_\alpha$ is a multivariate log-normal distribution with mean and covariance matrix given by

$$\begin{aligned} \mu_{LN,\alpha} &= \mathbb{E}\left(\exp(\alpha)|\mu_\alpha, \Sigma_\alpha\right) \quad \text{and} \quad \Sigma_{LN,\alpha} = \mathbb{V}\left(\exp(\alpha)|\mu_\alpha, \Sigma_\alpha\right) \quad \text{so that} \\ \mu_{LN,\alpha,i} &:= (\mu_{LN,\alpha})_i = \exp\left(\mu_{\alpha,i} + \frac{1}{2}\Sigma_{\alpha,ii}\right) \quad \text{and} \\ \Sigma_{LN,\alpha,ik} &:= (\Sigma_{LN,\alpha})_{ik} = \exp(\mu_{\alpha,i} + \mu_{\alpha,k} + 0.5(\Sigma_{\alpha,ii} + \Sigma_{\alpha,jj})) \exp(\Sigma_{\alpha,ik} - 1) \end{aligned} \quad (7)$$

The hierarchical prior given by Eq. (3) - Eq. (6) has some the important modeling advantage over previous priors for the random effects in the LBA model because it allows the random effects to be apriori correlated, with the parameters of the prior estimated from the data. The second improvement is that we use the marginally non-informative prior of Huang and Wand (2013) for the variance-covariance matrix as opposed to usual inverse Wishart prior. The extra information assumed in the inverse Wishart prior may not always be well justified.

3 Bayesian Estimation

This section discusses efficient Bayesian inference for the hierarchical LBA model described in Section 2.1. We use the particle MCMC approach of Gunawan et al. (2017) and also develop an annealed importance sampling approach for this model which is based on particle MCMC.

Let $\theta \in \Theta \subset R^{d_\theta}$ be the vector of unknown model parameters and let $p(\theta)$ be the prior for θ . Let \mathbf{y}_j be the vector of observations for the j th subject, and define $\mathbf{y} = \mathbf{y}_{1:S} = (\mathbf{y}_1, \dots, \mathbf{y}_S)$ as the vector of observations for all S subjects. Let $\alpha_j \in \chi_\alpha \subset R^{d_\alpha}$ be the vector of individual level parameters (random effects) for subject j , and $p(\alpha_j|\theta)$ its density. Now define $\alpha = \alpha_{1:S} = (\alpha_1, \dots, \alpha_S)$ as the vector of all individual level parameters. We assume that

$$p(\alpha_{1:S}|\theta) = \prod_{i=1}^S p(\alpha_i|\theta) \quad \text{and} \quad p(\mathbf{y}|\theta, \alpha) = \prod_{j=1}^S p(\mathbf{y}_j|\alpha_j, \theta),$$

so that the likelihood is

$$p(\mathbf{y}|\boldsymbol{\theta}) = \prod_{j=1}^S p(\mathbf{y}_j|\boldsymbol{\theta}) \quad \text{with} \quad p(\mathbf{y}_j|\boldsymbol{\theta}) = \int p(\mathbf{y}_j|\boldsymbol{\alpha}_j, \boldsymbol{\theta}) p(\boldsymbol{\alpha}_j|\boldsymbol{\theta}) d\boldsymbol{\alpha}_j. \quad (8)$$

Section 2.1 describes how to compute the densities $p(\mathbf{y}_{1:S}|\boldsymbol{\theta}, \boldsymbol{\alpha}_{1:S})$, $p(\boldsymbol{\alpha}_{1:S}|\boldsymbol{\theta})$, and $p(\boldsymbol{\theta})$, as described in Section 2.1.

Our goal is to sample from the posterior density

$$\pi(\boldsymbol{\theta}, \boldsymbol{\alpha}_{1:S}) := p(\mathbf{y}_{1:S}|\boldsymbol{\theta}, \boldsymbol{\alpha}_{1:S}) p(\boldsymbol{\alpha}_{1:S}|\boldsymbol{\theta}) p(\boldsymbol{\theta}) / p(\mathbf{y}_{1:S}), \quad (9)$$

where

$$p(\mathbf{y}) = \int \int p(\mathbf{y}_{1:S}|\boldsymbol{\theta}, \boldsymbol{\alpha}_{1:S}) p(\boldsymbol{\alpha}_{1:S}|\boldsymbol{\theta}) p(\boldsymbol{\theta}) d\boldsymbol{\theta} d\boldsymbol{\alpha}_{1:S} \quad (10)$$

is the marginal likelihood. We are usually also interested in estimating posterior distributions of functions $\varphi(\boldsymbol{\theta}, \boldsymbol{\alpha}_{1:S})$ and the expectations of such functions with respect to the posterior, i. e.,

$$\mathbb{E}_\pi(\varphi) = \int \int \varphi(\boldsymbol{\theta}, \boldsymbol{\alpha}_{1:S}) \pi(\boldsymbol{\theta}, \boldsymbol{\alpha}_{1:S}) d\boldsymbol{\theta} d\boldsymbol{\alpha}_{1:S}, \quad (11)$$

as well as estimating the marginal likelihood in Eq. (10), which is used for model selection.

3.1 Particle Markov chain Monte Carlo (PMCMC)

The basis of our PMCMC approach is to define a target distribution on an augmented space that includes the parameters of the model and multiple copies of the individual random effects, which we describe as particles. Gunawan et al. (2017) derive two samplers based on the same augmented target distribution. The first is the Pseudo Marginal Metropolis-Hastings sampler and the second is the Particle Metropolis within Gibbs (PMwG) sampler. See Gunawan et al. for a more complete discussion. Our article focuses on the PMwG sampler.

Let $\{m_j(\boldsymbol{\alpha}_j|\boldsymbol{\theta}, \mathbf{y}_j); j = 1, \dots, S\}$ be a family of proposal densities that we use to approximate the conditional posterior densities $\{\pi(\boldsymbol{\alpha}_j|\boldsymbol{\theta}); j = 1, \dots, S\}$. We define

$$\mathcal{S}_j^\theta := (\boldsymbol{\alpha}_j \in \mathcal{X}_\alpha : \pi(\boldsymbol{\alpha}_j|\boldsymbol{\theta}) > 0) \quad \text{and} \quad \mathcal{Q}_j^\theta := \{\boldsymbol{\alpha}_j \in \mathcal{X}_\alpha : m_j(\boldsymbol{\alpha}_j|\boldsymbol{\theta}, \mathbf{y}_j) > 0\}.$$

We assume that $\mathcal{S}_j^\theta \subseteq \mathcal{Q}_j^\theta$ for any $\boldsymbol{\theta} \in \boldsymbol{\Theta}$ and $j = 1, \dots, S$. This ensures that the proposal densities $m_j(\boldsymbol{\alpha}_j|\boldsymbol{\theta}, \mathbf{y}_j)$ can be used to approximate $\pi(\boldsymbol{\alpha}_j|\boldsymbol{\theta})$ defined on the spaces \mathcal{X}_α , for $j = 1, \dots, S$.

If we allow R particles (copies) of each vector of individual-level parameters in the random effects model, then the generic Monte Carlo sampling scheme (Algorithm 1) is

Algorithm 1 Monte Carlo Algorithm

For $j = 1, \dots, S$

1. Sample α_j^r from $m_j(\alpha_j | \theta, \mathbf{y}_j)$, for $r = 1, \dots, R$.
 2. Compute the weights $\tilde{w}_j^r = \frac{p(\mathbf{y}_j | \alpha_j^r, \theta) p(\alpha_j^r | \theta)}{m_j(\alpha_j^r | \theta, \mathbf{y}_j)}$, for $r = 1, \dots, R$.
 3. Normalise the weights $\tilde{W}_j^r = \frac{\tilde{w}_j^r}{\sum_{k=1}^R \tilde{w}_j^k}$, for $r = 1, \dots, R$.
-

To define the joint distribution of the particles given the parameters, let $\alpha_{1:S}^{1:R} := \{\alpha_1^{1:R}, \dots, \alpha_S^{1:R}\}$ and $\alpha_j^{1:R} := \{\alpha_j^1, \dots, \alpha_j^R\}$. The joint distribution is

$$\psi^\theta(\alpha_{1:S}^{1:R}) = \prod_{r=1}^R \prod_{j=1}^S m_j(\alpha_j^r | \theta, \mathbf{y}_j). \quad (12)$$

Algorithm 1 yields the following approximations to $\pi(d\alpha_{1:S} | \theta)$ and the unbiased estimator of the likelihood $p(\mathbf{y} | \theta)$

$$\hat{\pi}_R(d\alpha_{1:S} | \theta) := \prod_{j=1}^S \left\{ \sum_{r=1}^R \tilde{W}_j^r \delta_{\alpha_j^r}(d\alpha_j) \right\}, \quad \hat{p}_R(\mathbf{y} | \theta) = \prod_{j=1}^S \left(\frac{1}{R} \sum_{r=1}^R \tilde{w}_j^r \right).$$

To define the required augmented target densities, let $\mathbf{k} = (k_1, \dots, k_S)$, with each $k_j \in \{1, \dots, R\}$, $\alpha_{1:S}^{\mathbf{k}} = (\alpha_1^{k_1}, \dots, \alpha_S^{k_S})$ is a vector of all selected individual random effects, and $\alpha_{1:S}^{(-\mathbf{k})} = \{\alpha_1^{(-k_1)}, \dots, \alpha_S^{(-k_S)}\}$ is a collection of all particles excluding the selected individual random effects with $\alpha_j^{(-k_j)} = (\alpha_j^1, \dots, \alpha_j^{k_j-1}, \alpha_j^{k_j+1}, \dots, \alpha_j^R)$. We define the augmented target density

$$\tilde{\pi}_R(\theta, \alpha_{1:S}^{1:R}, \mathbf{k}) = \frac{\pi(\theta, \alpha_{1:S}^{\mathbf{k}})}{R^S} \frac{\psi^\theta(\alpha_{1:S}^{1:R})}{\prod_{j=1}^S m_j(\alpha_j^{k_j} | \theta, \mathbf{y}_j)}. \quad (13)$$

Gunawan et al. (2017) shows that the marginal density $\tilde{\pi}_R(\theta, \alpha_{1:S}^{1:R}, \mathbf{k}) = R^{-S} \pi(\theta, \alpha_{1:S}^{\mathbf{k}})$ using the target density in Eq. (13) and gives convergence results for the PMwG sampler.

Conditional Monte Carlo Algorithm

The expression

$$\frac{\psi^{\boldsymbol{\theta}}(\boldsymbol{\alpha}_{1:S}^{1:R})}{\prod_{j=1}^S m_j(\boldsymbol{\alpha}_j^{k_j} | \boldsymbol{\theta}, \mathbf{y}_j)}$$

appearing in the augmented target density in Eq. (13) is the density of all the particles that are generated by the Monte Carlo algorithm conditional on $(\boldsymbol{\alpha}_{1:S}^k, \mathbf{k})$. This is an important element in the PMwG algorithm. We can understand this step as updating $R - 1$ particles simultaneously while keeping one particle fixed in $\tilde{\pi}_R(\boldsymbol{\alpha}_{1:S}^{1:R} | \boldsymbol{\theta})$. Algorithm 2 gives the conditional Monte Carlo algorithm.

Algorithm 2 Conditional Monte Carlo Algorithm

1. Fix $\boldsymbol{\alpha}_{1:S}^1 = \boldsymbol{\alpha}_{1:S}^k$.
 2. For $j = 1, \dots, S$
 - (a) Sample $\boldsymbol{\alpha}_j^r$ from $m_j(\boldsymbol{\alpha}_j | \boldsymbol{\theta}, \mathbf{y}_j)$ for $r = 2, \dots, R$.
 - (b) Compute the importance weights $\tilde{w}_j^r = \frac{p(\mathbf{y}_j | \boldsymbol{\alpha}_j^r, \boldsymbol{\theta}) p(\boldsymbol{\alpha}_j^r | \boldsymbol{\theta})}{m_j(\boldsymbol{\alpha}_j^r | \boldsymbol{\theta}, \mathbf{y}_j)}$, for $r = 1, \dots, R$.
 - (c) Normalise the weights $\tilde{W}_j^r = \frac{\tilde{w}_j^r}{\sum_{k=1}^R \tilde{w}_j^k}$, for $r = 1, \dots, R$.
-

Particle Metropolis within Gibbs (PMwG) Sampling

We use the augmented target density in Eq. (13) in order to sample from $\pi(\boldsymbol{\theta}, \boldsymbol{\alpha}_{1:S}^k)$. Let $\boldsymbol{\theta} = (\boldsymbol{\theta}_1, \dots, \boldsymbol{\theta}_B)$ be a partition of the parameter vector $\boldsymbol{\theta}$ into B components. We use the notation $\boldsymbol{\theta}_{-b} := (\boldsymbol{\theta}_1, \dots, \boldsymbol{\theta}_{b-1}, \boldsymbol{\theta}_{b+1}, \dots, \boldsymbol{\theta}_B)$. The Particle Metropolis within Gibbs (PMwG) algorithm involves following steps.

Algorithm 3 Particle Metropolis within Gibbs (PMwG) Algorithm

1. For $b = 1, \dots, B$

(a) Sample $\boldsymbol{\theta}_b^*$ from the proposal $q_b(\cdot | \mathbf{k}, \boldsymbol{\alpha}_{1:S}^k, \boldsymbol{\theta}_b, \boldsymbol{\theta}_{-b})$

(b) Set $\boldsymbol{\theta}_b = \boldsymbol{\theta}_b^*$ with probability

$$\min \left\{ 1, \frac{\tilde{\pi}_R(\boldsymbol{\theta}_b^* | \mathbf{k}, \boldsymbol{\alpha}_{1:S}^k, \boldsymbol{\theta}_{-b})}{\tilde{\pi}_R(\boldsymbol{\theta}_b | \mathbf{k}, \boldsymbol{\alpha}_{1:S}^k, \boldsymbol{\theta}_{-b})} \times \frac{q_b(\boldsymbol{\theta}_b | \mathbf{k}, \boldsymbol{\alpha}_{1:S}^k, \boldsymbol{\theta}_b^*, \boldsymbol{\theta}_{-b})}{q_b(\boldsymbol{\theta}_b^* | \mathbf{k}, \boldsymbol{\alpha}_{1:S}^k, \boldsymbol{\theta}_b, \boldsymbol{\theta}_{-b})} \right\},$$

2. Sample $\boldsymbol{\alpha}_{1:S}^{(-\mathbf{k})} \sim \tilde{\pi}_R(\cdot | \mathbf{k}, \boldsymbol{\alpha}_{1:S}^k, \boldsymbol{\theta})$ using the conditional Monte Carlo algorithm in Algorithm 2.

3. Sample the index vector $\mathbf{k} = (k_1, \dots, k_S)$ with probability given by

$$\tilde{\pi}_R(k_1 = l_1, \dots, k_S = l_S | \boldsymbol{\theta}, \boldsymbol{\alpha}_{1:S}^{1:R}) = \prod_{j=1}^S \widetilde{W}_j^{l_j},$$

Algorithm 4 describes the PMwG sampling scheme, making explicit those details that are specific to the LBA model. Steps (2a), (2b), and (2c) sample the parameters of the LBA model. Step (2a) samples $\boldsymbol{\mu}_\alpha$ from its full conditional posterior by drawing from $N(\bar{\boldsymbol{\mu}}, \bar{\boldsymbol{\Sigma}})$, where $\bar{\boldsymbol{\Sigma}} = (S\boldsymbol{\Sigma}_\alpha^{-1} + I)^{-1}$ and $\bar{\boldsymbol{\mu}} = \bar{\boldsymbol{\Sigma}} \left(\boldsymbol{\Sigma}_\alpha^{-1} \sum_{j=1}^S \boldsymbol{\alpha}_j \right)$. Step 2(b) samples $\boldsymbol{\Sigma}_\alpha$ by drawing from $IW(k_\alpha, \mathbf{B}_\alpha)$, where $k_\alpha = v_\alpha + D_\alpha - 1 + S$, $\mathbf{B}_\alpha = 2v_\alpha \text{diag}(1/a_1, \dots, 1/a_{D_\alpha}) + \sum_{j=1}^S (\boldsymbol{\alpha}_j - \boldsymbol{\mu}_\alpha)(\boldsymbol{\alpha}_j - \boldsymbol{\mu}_\alpha)^\top$. Step (2c) samples the parameters a_d from $IG\left(\frac{v_\alpha + D_\alpha}{2}, v_\alpha(\boldsymbol{\Sigma}_\alpha^{-1})_{dd} + \frac{1}{\mathcal{A}_d^2}\right)$ for $d = 1, \dots, D_\alpha$. In step (3), we run the conditional Monte Carlo algorithm to obtain the $\boldsymbol{\alpha}_{1:S}^{(-\mathbf{k})}$, and, finally, we sample the index vector $\mathbf{k} = (k_1, \dots, k_S)$. Note that, steps (2a) - (2c) in the conditional Monte Carlo in Algorithm 2 can easily be parallelised for $r = 1, \dots, R$. This is one of the main advantages of the PMwG approach. Section 3.2 discusses our AISIL-RE approach which implements the Markov step based on this PMwG algorithm.

Algorithm 4 PMwG Algorithm for the LBA Model

1. Select initial values for $\boldsymbol{\alpha}$, \mathbf{k} , and $\boldsymbol{\theta}$,
2. (a) Sample $\boldsymbol{\mu}_\alpha | \mathbf{k}, \boldsymbol{\alpha}_{1:S}^k, \boldsymbol{\theta}_{-\mu_\alpha}$ from $N(\bar{\boldsymbol{\mu}}, \bar{\boldsymbol{\Sigma}})$, where $\bar{\boldsymbol{\Sigma}} = (S\boldsymbol{\Sigma}_\alpha^{-1} + I)^{-1}$ and $\bar{\boldsymbol{\mu}} = \bar{\boldsymbol{\Sigma}} \left(\boldsymbol{\Sigma}_\alpha^{-1} \sum_{j=1}^S \boldsymbol{\alpha}_j \right)$
 (b) Sample $\boldsymbol{\Sigma}_\alpha | \mathbf{k}, \boldsymbol{\alpha}_{1:S}^k, \boldsymbol{\theta}_{-\Sigma_\alpha}$ from $IW(k_\alpha, \mathbf{B}_\alpha)$, where $k_\alpha = v_\alpha + D_\alpha - 1 + S$ and $\mathbf{B}_\alpha = 2v_\alpha \text{diag}(1/a_1, \dots, 1/a_D) + \sum_{j=1}^S (\boldsymbol{\alpha}_j - \boldsymbol{\mu}_\alpha)(\boldsymbol{\alpha}_j - \boldsymbol{\mu}_\alpha)^\top$.
 (c) Sample $a_d | \mathbf{k}, \boldsymbol{\alpha}_{1:S}^k, \boldsymbol{\theta}_{-a_d}$ from $IG\left(\frac{v_\alpha + D_\alpha}{2}, v_\alpha (\boldsymbol{\Sigma}_\alpha^{-1})_{dd} + \frac{1}{\mathcal{A}_d^2}\right)$ for $d = 1, \dots, D$.
3. Sample $\boldsymbol{\alpha}_{1:S}^{(-\mathbf{k})} \sim \tilde{\pi}_R(\cdot | \mathbf{k}, \boldsymbol{\alpha}_{1:S}^{(\mathbf{k})}, \boldsymbol{\theta})$ using the conditional Monte Carlo algorithm (Algorithm 2).
4. Sample the index vector $\mathbf{k} = (k_1, \dots, k_S)$ with probability given by

$$\tilde{\pi}_R(k_1 = l_1, \dots, k_S = l_S | \boldsymbol{\theta}, \boldsymbol{\alpha}_{1:S}^{1:R}) = \prod_{j=1}^S \widetilde{W}_j^{l_j},$$

Tuning parameters and proposal densities for the PMwG sampler

For the PMwG method, we must specify the number of particles R , and the proposal densities $m_j(\boldsymbol{\alpha}_j | \boldsymbol{\theta}, \mathbf{y}_j)$, for each subject $j = 1, \dots, S$. Gunawan et al. (2017) use the prior densities $p(\boldsymbol{\alpha}_j | \boldsymbol{\mu}_\alpha, \boldsymbol{\Sigma}_\alpha)$ as the proposal densities for the random effects for each subject $j = 1, \dots, S$. We have explored this, and found that the sampler works quite well that way, but slowly. We have developed a more efficient approach, extending Gunawan et al.'s by proposing more efficient proposal densities for the random effects for each subject $j = 1, \dots, S$.

The more efficient proposal densities are developed in three stages of sampling: burn in, initial adaptation, and sampling. The PMwG sampler starts at a specified initial set of parameters $\boldsymbol{\theta} = (\boldsymbol{\mu}_\alpha, \boldsymbol{\Sigma}_\alpha)$ and random effects $\boldsymbol{\alpha}$. Then, the PMwG sampler proceeds as in Algorithm 4.

Initially, in the burn-in and the initial adaptation stages, the proposal density for subject j is the two component mixture

$$m_j(\boldsymbol{\alpha}_j | \boldsymbol{\theta}, \mathbf{y}_j) = w_{mix} N(\boldsymbol{\alpha}_j; \boldsymbol{\alpha}_j^{(iter-1)}, \boldsymbol{\Sigma}_\alpha) + (1 - w_{mix}) p(\boldsymbol{\alpha}_j | \boldsymbol{\mu}_\alpha, \boldsymbol{\Sigma}_\alpha), \quad (14)$$

where $\boldsymbol{\alpha}_j^{(iter-1)}$ is the previous sample for the individual random effects. We use a

larger number of particles $R_{adapt} = 1000$ in the burn in and the initial adaptation stages, and set $w_{mix} = 0.5$.

In the sampling stage, we use the posterior MCMC draws $(\boldsymbol{\alpha}_j, \boldsymbol{\theta})$ for $j = 1, \dots, S$ from the initial adaptation stage to the previous iteration of the PMwG sampler to adaptively build more efficient proposal densities $m_j(\boldsymbol{\alpha}_j | \boldsymbol{\theta}, \mathbf{y}_j)$, for each subject $j = 1, \dots, S$. This allows the use of a much smaller number of particles: $R_{sampling} = 100$. We first transform the posterior draws of the parameters $\boldsymbol{\Sigma}_\alpha$ so that they all lie on the real line. The covariance matrix $\boldsymbol{\Sigma}$ is reparameterised in terms of its Cholesky factorisation $\boldsymbol{\Sigma} = \mathbf{L}\mathbf{L}^T$, where \mathbf{L} is a lower triangular matrix. We also apply a log transformation for the diagonal elements of the \mathbf{L} . The elements below the diagonal of \mathbf{L} are unrestricted. We fit a normal distribution to the posterior draws of $\boldsymbol{\alpha}_j$ and $(\boldsymbol{\mu}, \mathbf{L})$ and obtain the conditional distribution $g(\boldsymbol{\alpha}_j | \boldsymbol{\mu}, \mathbf{L}) \sim N(\boldsymbol{\alpha}_j; \boldsymbol{\mu}_{j,prop}, \boldsymbol{\Sigma}_{j,prop})$ for $j = 1, \dots, S$. The efficient proposal density for subject j is then the two component mixture

$$m_j(\boldsymbol{\alpha}_j | \boldsymbol{\theta}, \mathbf{y}_j) = w_{mix} N(\boldsymbol{\alpha}_j; \boldsymbol{\mu}_{j,prop}, \boldsymbol{\Sigma}_{j,prop}) + (1 - w_{mix}) p(\boldsymbol{\alpha}_j | \boldsymbol{\theta}). \quad (15)$$

Following Hesterberg (1995), the inclusion of the prior density $p(\boldsymbol{\alpha}_j | \boldsymbol{\theta})$ in Eq. (14) and Eq. (15) ensures that the importance weights are bounded given that the conditional likelihood $p(\mathbf{y}_j | \boldsymbol{\theta}, \boldsymbol{\alpha}_j)$ is bounded. The proof that the conditional likelihood $p(\mathbf{y}_j | \boldsymbol{\theta}, \boldsymbol{\alpha}_j)$ is bounded is given in Appendix C. We set the mixture weight $w_{mix} = 0.9$ in the sampling stage.

3.2 Annealed Importance Sampling with an Intractable Likelihood for the random effects model (AISIL-RE)

The AISIL-RE method builds upon the AIS algorithm of Neal (2001) to construct a sequence of annealed target densities and uses a version of the sequential Monte-Carlo sampler of Del Moral et al. (2006) to draw from this sequence. AISIL-RE propagates a particle cloud $(\boldsymbol{\theta}_{1:M}^{(p)}, \boldsymbol{\alpha}_{1:M}^{(p)}, W_{1:M}^{(p)})$ through a sequence of tempered target densities $\xi_{a_p}(\boldsymbol{\theta}, \boldsymbol{\alpha})$, for $p = 0, \dots, P$, to the posterior density of interest, $\pi(\boldsymbol{\theta}, \boldsymbol{\alpha})$, which is much harder to sample directly. The tempered densities are defined as

$$\xi_{a_p}(\boldsymbol{\theta}, \boldsymbol{\alpha}) = \eta_{a_p}(\boldsymbol{\theta}, \boldsymbol{\alpha}) / Z_{a_p}, \quad \text{with} \quad Z_{a_p} = \int \eta_{a_p}(\boldsymbol{\theta}, \boldsymbol{\alpha}) d\boldsymbol{\theta} d\boldsymbol{\alpha} \quad (16)$$

where

$$\eta_{a_p}(\boldsymbol{\theta}, \boldsymbol{\alpha}) = (\pi_0(\boldsymbol{\theta}, \boldsymbol{\alpha}))^{1-a_p} (p(\mathbf{y} | \boldsymbol{\theta}, \boldsymbol{\alpha}) p(\boldsymbol{\alpha} | \boldsymbol{\theta}) p(\boldsymbol{\theta}))^{a_p}.$$

The AISIL-RE algorithm produces the M triples $(\boldsymbol{\theta}_m^{(P)}, \boldsymbol{\alpha}_m^{(P)}, W_m^{(P)})$ for $m =$

$1, \dots, M$ which approximates the posterior distribution of interest $\pi(\boldsymbol{\theta}, \boldsymbol{\alpha})$. The tempering sequence $a_{0:P}$ is such that $a_0 = 0 < a_1 < \dots < a_P = 1$. If it is both easy to generate and evaluate the densities of $p(\boldsymbol{\theta})$ and $p(\boldsymbol{\alpha}|\boldsymbol{\theta})$, then we take $\pi_0(\boldsymbol{\theta}, \boldsymbol{\alpha}) = p(\boldsymbol{\theta})p(\boldsymbol{\alpha}|\boldsymbol{\theta})$, and then

$$\eta_{a_p}(\boldsymbol{\theta}, \boldsymbol{\alpha}) = p(\mathbf{y}|\boldsymbol{\theta}, \boldsymbol{\alpha})^{a_p} p(\boldsymbol{\alpha}|\boldsymbol{\theta}) p(\boldsymbol{\theta}).$$

Algorithm 5 describes the AISIL-RE algorithm. Steps (1), (2a)-(2d) are standard and apply to any model with slight modification. Step (2e) does L Markov steps based on the PMwG algorithm for the LBA model. The Markov move is based on Algorithm 4 except that in Step 2 we sample $\boldsymbol{\alpha}_{1:S}^{(-\mathbf{k})} \sim \tilde{\xi}_{a_p}(\cdot|\mathbf{k}, \boldsymbol{\alpha}_{1:S}^{(\mathbf{k})}, \boldsymbol{\theta})$ using the conditional Monte Carlo (Algorithm 6).

At the initial temperature, the particle cloud $\{\boldsymbol{\theta}_{1:M}^{(0)}, \boldsymbol{\alpha}_{1:M}^{(0)}, W_{1:M}^{(0)}\}$ is obtained by sampling $\{\boldsymbol{\theta}_{1:M}^{(0)}, \boldsymbol{\alpha}_{1:M}^{(0)}\}$ from $\pi_0(\boldsymbol{\alpha}, \boldsymbol{\theta})$, and gives all particles equal weight, $W_{1:M}^{(0)} = 1/M$. The particle cloud $\{\boldsymbol{\theta}_{1:M}^{(p-1)}, \boldsymbol{\alpha}_{1:M}^{(p-1)}, W_{1:M}^{(p-1)}\}$ at the $(p-1)$ st iteration is an estimate of the $\xi_{a_{p-1}}(\boldsymbol{\theta}, \boldsymbol{\alpha})$. We implement the transition from the particle cloud estimate of $\xi_{a_{p-1}}(\boldsymbol{\theta}, \boldsymbol{\alpha})$ to the particle cloud estimate $\xi_{a_p}(\boldsymbol{\theta}, \boldsymbol{\alpha})$ by first reweighting the $(p-1)$ st cloud of particles to obtain the updated weights

$$W_{1:M}^{(p)} = \frac{w_{1:M}}{\sum_{j=1}^M w_j}, \text{ where } w_m^{(p)} = W_m^{(p-1)} \frac{\eta_{a_p}(\boldsymbol{\theta}_m, \boldsymbol{\alpha}_m)}{\eta_{a_{p-1}}(\boldsymbol{\theta}_m, \boldsymbol{\alpha}_m)} = W_m^{(p-1)} p(\mathbf{y}|\boldsymbol{\theta}_m, \boldsymbol{\alpha}_m)^{a_p - a_{p-1}}.$$

We then follow Del Moral et al. (2012) and select the next value of a_p to target a pre-defined effective sample size ESS_T^1 . We do so by evaluating the ESS over a grid points $a_{1:G,p}$ of potential a_p values and select as a_p the value of $a_{j,p}$ whose ESS is the closest to ESS_T . After reweighting, the effective sample size (ESS) is reduced to a value close to ESS_T . To eliminate particles with low weight and replicate particles with larger weights, $\{\boldsymbol{\theta}_{1:M}^{(p)}, \boldsymbol{\alpha}_{1:M}^{(p)}\}$ are resampled with probabilities given by their normalised weights. Repeated application of this procedure can reduce the particle diversity so that the particle cloud at the p th iteration may not be a good approximation to $\xi_{a_p}(\boldsymbol{\theta}, \boldsymbol{\alpha})$. To improve the approximation, we carry out L Markov move steps for each particle, using a Markov kernel $K_{\xi_{a_p}}$ that is based on the PMwG algorithm, and has ξ_{a_p} as its invariant density.

We now define the augmented tempered target densities for each of the annealing step. For $R \geq 1$, AISIL-RE constructs a sequence of tempered densities $\xi_{a_p}(\boldsymbol{\theta}, \boldsymbol{\alpha}_{1:S}^{\mathbf{k}})$,

¹ESS stands for the effective sample size and is used to measure the weight variability. It is defined as $\text{ESS} = \frac{1}{\sum_{i=1}^M (W_i^{(p-1)})^2}$, and varies between 1 and M , where a low value of ESS indicates that the weights are concentrated only on a few particles.

Algorithm 5 The AISIL-RE Algorithm

1. Set $p = 0$ and generate $\{\boldsymbol{\theta}_{1:M}^{(0)}, \boldsymbol{\alpha}_{1:M}^{(0)}, W_{1:M}^{(0)}\}$ from $\pi_0(\boldsymbol{\alpha}, \boldsymbol{\theta})$, and give them equal weight, i.e., $W_m^{(0)} = 1/M$, for $m = 1, \dots, M$
2. While the tempering sequence $a_p < 1$ do
 - (a) Set $p \leftarrow p + 1$
 - (b) Find a_p adaptively by searching across a grid of a_p to maintain effective sample size near some constant ESS_T .
 - (c) Compute new weights,

$$W_{1:M}^{(p)} = \frac{w_{1:M}}{\sum_{j=1}^M w_j} \text{ where } w_m^{(p)} = W_m^{(p-1)} \frac{\eta_{a_p}(\boldsymbol{\theta}_m, \boldsymbol{\alpha}_m)}{\eta_{a_{p-1}}(\boldsymbol{\theta}_m, \boldsymbol{\alpha}_m)} = W_m^{(p-1)} p(\mathbf{y}|\boldsymbol{\theta}_m, \boldsymbol{\alpha}_m)^{a_p - a_{p-1}}.$$

- (d) Resample $(\boldsymbol{\theta}_m^{(p)}, \boldsymbol{\alpha}_m^{(p)})$ using the weights $W_{1:M}^{(p)}$ to obtain $\{\boldsymbol{\theta}_{1:M}^{(p)}, \boldsymbol{\alpha}_{1:M}^{(p)}, W_{1:M}^{(p)} = 1/M\}$.
 - (e) Make L Markov moves
 - i. Let $K_{a_p}((\boldsymbol{\theta}, \boldsymbol{\alpha}), \cdot)$ be a Markov kernel having invariant density $\xi_{a_p}(\boldsymbol{\theta}, \boldsymbol{\alpha})$. For $m = 1, \dots, M$, move each $(\boldsymbol{\theta}_m^{(p)}, \boldsymbol{\alpha}_m^{(p)})$ L times using the Markov kernel K_{a_p} to obtain $\{\tilde{\boldsymbol{\theta}}_m, \tilde{\boldsymbol{\alpha}}_m\}$. The Markov move step is based on PMwG sampling scheme in Algorithm 3, except that instead of $\tilde{\pi}_R$, we have augmented tempered target densities $\tilde{\xi}_{a_p}$.
 - ii. Set $(\boldsymbol{\theta}_{1:M}^{(p)}, \boldsymbol{\alpha}_{1:M}^{(p)}) \leftarrow (\tilde{\boldsymbol{\theta}}_{1:M}, \tilde{\boldsymbol{\alpha}}_{1:M})$ and set $W_{1:M}^{(p)} = 1/M$.
-

$p = 0, \dots, P$, based on the augmented tempered target density

$$\tilde{\xi}_{a_p}(\boldsymbol{\theta}, \boldsymbol{\alpha}_{1:S}^{1:R}, \mathbf{k}) = \frac{\xi_{a_p}(\boldsymbol{\theta}, \boldsymbol{\alpha}_{1:S}^{\mathbf{k}})}{R^S} \frac{\psi^{\boldsymbol{\theta}}(\boldsymbol{\alpha}_{1:S}^{1:R})}{\prod_{j=1}^S m_j(\boldsymbol{\alpha}_j^{\mathbf{k}_j} | \boldsymbol{\theta}, \mathbf{y}_j)}, \quad (17)$$

where Eq. (12) gives $\psi^{\boldsymbol{\theta}}(\boldsymbol{\alpha}_{1:S}^{1:R})$.

Using the same derivation as in Gunawan et al. (2017), we can show that $R^{-S} \xi_{a_p}(\boldsymbol{\theta}, \boldsymbol{\alpha}_{1:S}^{\mathbf{k}})$ is the marginal probability density of $\tilde{\xi}_{a_p}(\boldsymbol{\theta}, \boldsymbol{\alpha}_{1:S}^{1:R}, \mathbf{k})$. The tempered target densities $\xi_{a_p}(\boldsymbol{\theta}, \boldsymbol{\alpha}_{1:S}^{\mathbf{k}})$ are the marginal densities of the augmented tempered target densities in Eq. (17). The augmented tempered target densities also involves the term

$$\frac{\psi^{\boldsymbol{\theta}}(\boldsymbol{\alpha}_{1:S}^{1:R})}{\prod_{j=1}^S m_j(\boldsymbol{\alpha}_j^{\mathbf{k}_j} | \boldsymbol{\theta}, \mathbf{y}_j)},$$

which is the density under $\tilde{\xi}_{a_p}$ of all particles that are generated by the Monte-Carlo algorithm conditional on $(\boldsymbol{\alpha}_{1:S}^{1:R}, \mathbf{k})$. Note that the Monte-Carlo and conditional Monte-Carlo algorithms are similar to the one given in Algorithms 1 and 2, respectively, except that the AISIL versions adopt the tempered conditional likelihood $p(\mathbf{y}|\boldsymbol{\theta}, \boldsymbol{\alpha})^{a_p}$ instead of $p(\mathbf{y}|\boldsymbol{\theta}, \boldsymbol{\alpha})$. Furthermore, the Markov move step is based on the PMwG sampling scheme in Algorithm 3, except that instead of $\tilde{\pi}_R$, we have augmented tempered target densities $\tilde{\xi}_{a_p}$.

Algorithm 6 Conditional Monte Carlo Algorithm in the AISIL-RE algorithm

1. Fix $\boldsymbol{\alpha}_{1:S}^1 = \boldsymbol{\alpha}_{1:S}^k$.
 2. For $j = 1, \dots, S$,
 - (a) Sample $\boldsymbol{\alpha}_j^r$ from $m_j(\cdot|\boldsymbol{\theta}, \mathbf{y}_j)$ for $r = 2, \dots, R$.
 - (b) Compute the importance weights $\tilde{w}_j^r = \frac{p(\mathbf{y}_j|\boldsymbol{\alpha}_j^r, \boldsymbol{\theta})^{a_p} p(\boldsymbol{\alpha}_j^r|\boldsymbol{\theta})}{m_j(\boldsymbol{\alpha}_j^r|\boldsymbol{\theta}, \mathbf{y}_j)}$, for $r = 1, \dots, R$.
 - (c) Normalise the weights $\tilde{W}_j^r = \frac{\tilde{w}_j^r}{\sum_{k=1}^R \tilde{w}_j^k}$, for $r = 1, \dots, R$.
-

Discussion of the Tuning Parameters and Proposal Densities for the AISIL-RE algorithm

The AISIL-RE procedure has three tuning parameters: the number of particles R , the number of Markov move steps L , and the number of annealed samples M .

The higher the number of annealed samples M , the better the approximation of the posterior density of interest $\pi(\boldsymbol{\theta}, \boldsymbol{\alpha})$. By using the result of Del Moral et al. (2006), the AISIL-RE algorithm provides consistent inference for the posterior density $\pi(\boldsymbol{\theta}, \boldsymbol{\alpha})$ as the number of annealed samples M goes to infinity, for any given number of particles R . In our application, we set $M = 250$.

The L Markov moves in step (2e) in algorithm 5 help to diversify the collection of parameters and random effects after the resampling step in step (2d) so that they are better approximations to the tempered target density at that annealed temperature. Our AISIL-RE method implements Markov moves based on PMwG sampler with the conditional Monte Carlo algorithm given in Algorithm 6.

When the annealed temperature is small or close to zero, the tempered conditional likelihood is much flat (i.e., $p(\mathbf{y}_j|\boldsymbol{\theta}, \boldsymbol{\alpha}_j)^{a_p} \approx 1$), and the prior density $p(\boldsymbol{\alpha}_j|\boldsymbol{\theta})$ dominates the tempered conditional likelihood. For that reason, the prior density $p(\boldsymbol{\alpha}_j|\boldsymbol{\theta})$ is an efficient proposal for the random effects for each subject. In our application, we use the prior density as a proposal density when the annealed temperature

$a_p < 0.1$. We may use smaller number of particles R and smaller number of Markov steps L when the annealed temperature is small.

When the annealed temperature is larger than 0.1, we first fit a normal distribution to current particle cloud transformed LBA parameters and random effects $\{(\boldsymbol{\mu}, \mathbf{L})_{1:M}^{(p)}, \boldsymbol{\alpha}_{j,1:M}^{(p)}, W_{1:M}^{(p)}\}$ for $j = 1, \dots, S$ and obtain the conditional distribution $g(\boldsymbol{\alpha}_j | \boldsymbol{\mu}, \mathbf{L}) \sim N(\boldsymbol{\alpha}_j; \boldsymbol{\mu}_{j,prop}, \boldsymbol{\Sigma}_{j,prop})$ for $j = 1, \dots, S$ at each stage of annealing process. We then use two component mixture proposal given in Eq. (15) as a proposal density. We also set the mixture weight $w_{mix} = 0.9$. Note that AISIL-RE method does not require initial adaptation stage because we can obtain proposal densities of the random effects for each subject from the current particle cloud at each stage of annealing process.

At every stage of the annealing process, we can monitor the diversity of the parameters and random effects. If there are a lot of copies of the same parameters and random effects, this implies that the Markov moves are very inefficient. If all of the M annealed samples are different, that implies that the Markov moves are efficient. Our approach is that if we see a lot of copies of the same parameters and random effects, we then increase the number of particles R and the number of Markov moves L . In our empirical application, we set $R = 100$ and $L = 10$.

3.3 Estimating the Marginal Likelihood

The marginal likelihood $p(\mathbf{y})$ given in Eq. (10) is used in the Bayesian literature to compare between competing models (see Kass and Raftery 1995; Chib and Jeliazkov 2001). The AISIL method provides a convenient estimate of the marginal likelihood, as a by-product of computation. We note that $p(\mathbf{y}) = Z_{a_p}$ and $Z_{a_0} = 1$, so that

$$p(\mathbf{y}) = \prod_{p=1}^P \frac{Z_{a_p}}{Z_{a_{p-1}}} \quad \text{with} \quad \frac{Z_{a_p}}{Z_{a_{p-1}}} = \int \left(\frac{\eta_{a_p}(\boldsymbol{\theta}, \boldsymbol{\alpha})}{\eta_{a_{p-1}}(\boldsymbol{\theta}, \boldsymbol{\alpha})} \right) \tilde{\xi}_{a_{p-1}}(\boldsymbol{\theta}, \boldsymbol{\alpha}) d\boldsymbol{\theta} d\boldsymbol{\alpha}.$$

The particle cloud $(\boldsymbol{\theta}_{1:M}^{(p-1)}, \boldsymbol{\alpha}_{1:M}^{(p-1)}, W_{1:M}^{(p-1)})$ approximates $\tilde{\xi}_{a_{p-1}}(\boldsymbol{\theta}, \boldsymbol{\alpha})$, so that the ratio $Z_{a_p}/Z_{a_{p-1}}$ is estimated by,

$$\frac{\widehat{Z_{a_p}}}{Z_{a_{p-1}}} = \sum_{m=1}^M w_m^{(p)}$$

giving the marginal likelihood estimate as

$$\hat{p}(\mathbf{y}) = \prod_{p=1}^P \frac{\widehat{Z_{a_p}}}{Z_{a_{p-1}}}.$$

4 Illustrative Applications

4.1 Application to Simulated Data

This section applies the PMwG and AISIL-RE methods to fit the hierarchical LBA model specified in Section 2 with data simulated from an LBA model, mimicking conditions inspired by the experiment of Forstmann et al. (2008). We generated $N = 450$ trials (150 trials in each condition) from each of $S = 19$ subjects. Tables 1 (for means and variances of group-level distributions) and 2 (for their covariances) report the parameters values that generated the data under the columns headed “True”. We note that the data generating parameters included non-zero correlations between model parameters, within participants (the off-diagonal covariance elements of matrix Σ_α reported in Table 2).

There are three stages in our PMwG sampler: the burn in, the initial adaptation, and the sampling stages. The first 500 iterates were discarded as burn in. The length of the initial adaptation stage was set such that the draws of individual random effects for each subject have at least 20 unique values to estimate the initial covariance matrix Σ_{prop} . A total of 10000 draws were obtained in the sampling stages for the subsequent analysis. The number of Monte Carlo samples in the PMwG method was set to $R_{adapt} = 1,000$ and $R_{sampling} = 100$. We use the Integrated Autocorrelated Time (IACT), which measures inefficiency, to assess the performance of the PMwG sampler. For a univariate parameter ω , the IACT is defined as

$$\text{IACT}_\omega = 1 + 2 \sum_{t=1}^{\infty} \rho_\omega(t),$$

where $\rho_\omega(t)$ is the lag- t autocorrelation of the iterates of ω in the MCMC after the chain has converged. We use the CODA package of Plummer et al. (2006) to estimate the IACT values of the parameters. A low value of the IACT estimate suggests that the Markov chain mixed well, and so sampled efficiently.

For the AISIL-RE method, we ran 10 independent samplers with $M = 250$ samples each, to generate 2500 AISIL samples of the LBA individual random effects and parameters, and to obtain 10 independent log of the marginal likelihood estimates from which we can assess the variability of the estimates. The number of Monte-Carlo samples and Markov moves were set to $R = 100$ and $L = 10$. We set $ESS_T = 0.8M$; i.e., we targeted an effective sample size of 80% of the maximum annealing sample size.

The wall-clock computation time to run the PMwG and the AISIL-RE methods were 35.56 and 65.22 minutes, respectively using a Matlab implementation of the

algorithm and 28 CPU-cores of a high performance computer cluster. The running time for PMwG includes the burn in and the initial adaptation stages. The wall-clock computation time for the sampling stage was 20 minutes to obtain 10000 samples.

Figures 1 and 2 show the kernel density estimates of some of the LBA individual random effects and parameters based on PMwG and AISIL-RE samples. These figures show that the AISIL-RE estimates are very close to the PMwG estimates for all parameters, which provides a reassuring check. The estimated log of the marginal likelihood (with standard errors) is 2425.75(2.40). The standard error is small and this indicates that the log of the marginal likelihood is estimated accurately. For the subsequent analysis, we focus on the PMwG samples.

Tables 1 and 2 show the true values and the posterior means of the LBA parameters as well as their 95% credible intervals. The true values for most of the LBA parameters are within the 95% credible intervals. With more simulated observations, the estimates would be closer to the true values – there were only $S = 19$ simulated participants in this study. Figure 3 shows kernel density estimates of the marginal posterior densities of the individual-subject random effects parameters $\alpha_{v_j^{(2)}}$ and α_{A_j} for subjects $j = 1, 2, 11, 12$. The true values are within the 95% credible interval estimates.

Figure 4 shows the kernel density estimates of the marginal posterior densities of the $\boldsymbol{\mu}_{\alpha_b(1)}$, $\boldsymbol{\mu}_{\alpha_b(2)}$, and $\boldsymbol{\mu}_{\alpha_b(3)}$ as examples of the posterior distribution at the group level. There is considerable overlap between the three marginal distributions representing the different threshold parameters for the speed, neutral, and accuracy conditions. This may suggest that, even though the data are simulated as if there are three conditions in the experiments, the differences between the conditions, and the size of the sample, may better support a model with shared threshold parameters. This is exactly the kind of model selection question facing researchers using the LBA. We show in Section 4.2 how to use the marginal likelihood estimates obtained using AISIL to compare the unrestricted (three parameter) model against restricted models (with one or two shared parameters).

We evaluated the efficiency of the PMwG sampling method using inefficiency factors (IACT). Table 7, in Appendix A, reports IACT values for the group level parameters from the PMwG sampler. All the IACT of the group level parameters are small, which indicates that the chains mixed well. Figure 10 in Appendix A shows the distributions of IACT estimates for each subject’s random effect parameters, also for the PMwG method. Similar conclusions can be drawn from these random effects parameters as for the group-level parameters. There is also a single outlier for each of the random effects with poorer efficiency than the others. The outlier for all random effects parameters comes from the same simulated subject (subject 18). Even with

this reduced sampling efficiency for subject 18, Figure 5 shows that the true values of their particular individual random effect parameters of subject 18 are still within the posterior distribution estimates.

Figure 1: Kernel density estimates of some of the individual random effects parameters.

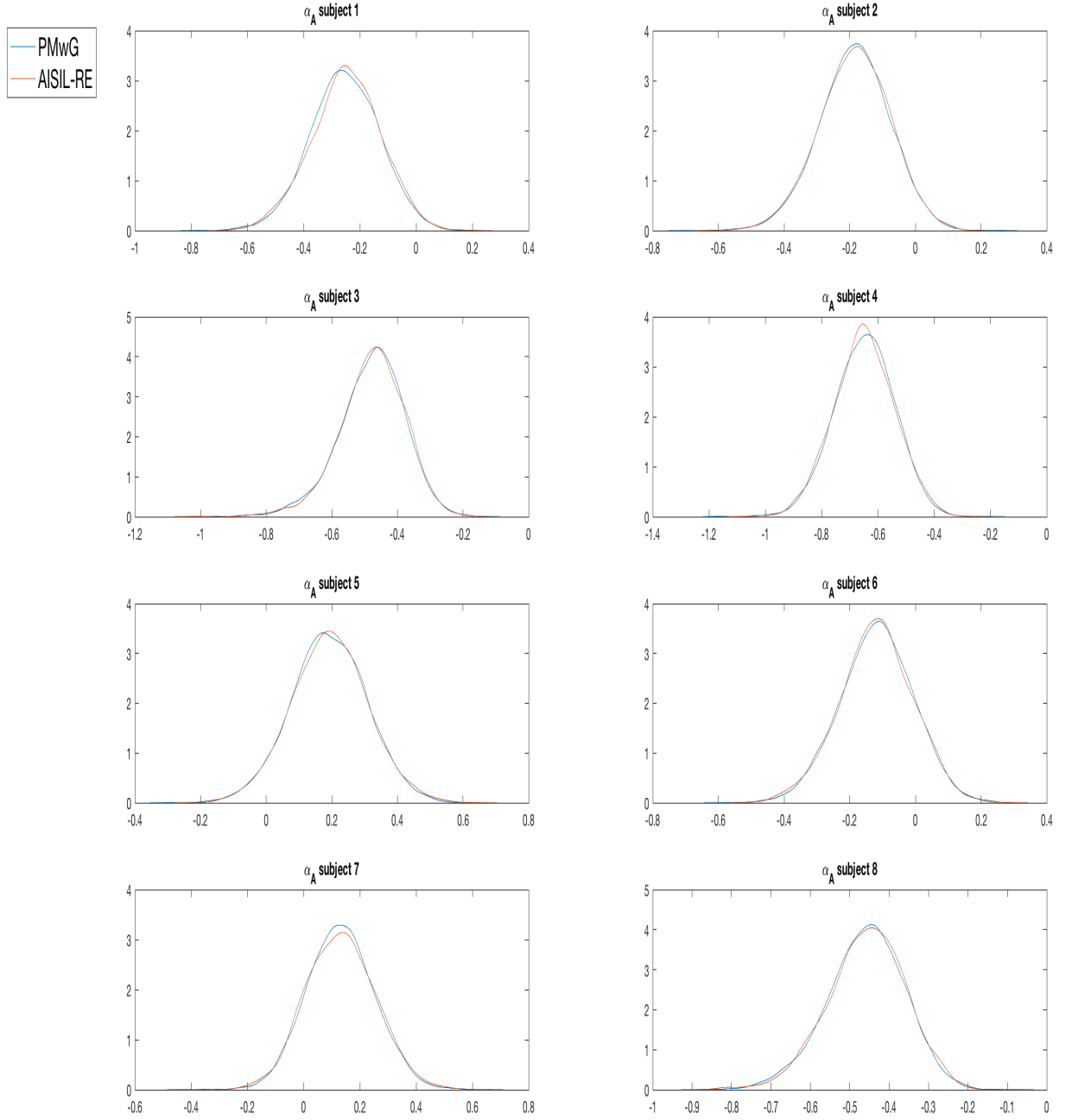


Figure 2: Kernel density estimates of some of the LBA parameters.

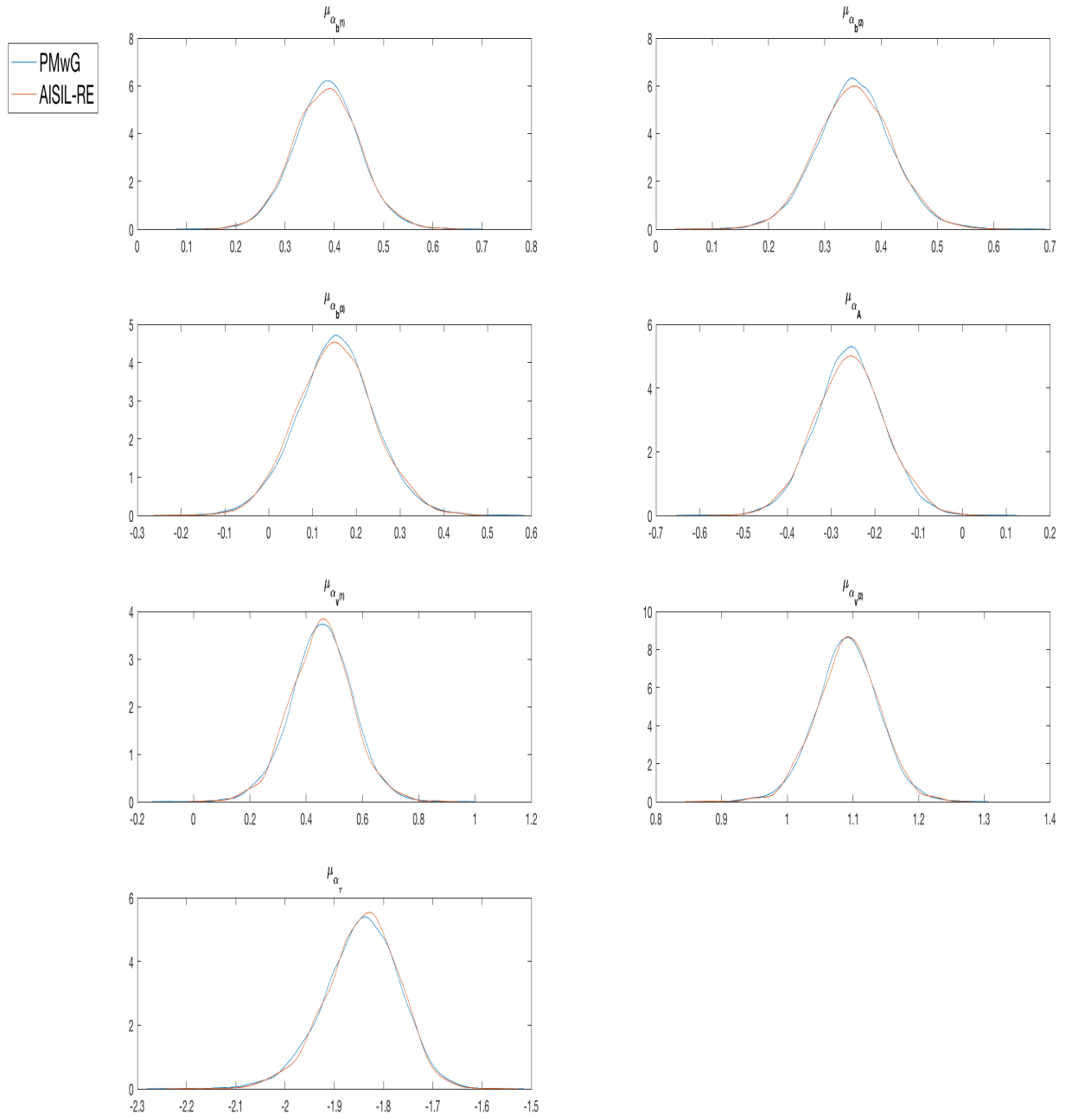


Table 1: Posterior Means with 95% credible intervals of the LBA parameters (all the μ_α and the diagonal elements of Σ_α) are estimated using the PMwG method in the simulation study.

Param	True	Est	Param.	True	Est
$\mu_{\alpha_b(1)}$	0.27	0.39 (0.25,0.52)	$\Sigma_{\alpha,11}$	0.06	0.07 (0.03,0.15)
$\mu_{\alpha_b(2)}$	0.22	0.35 (0.22,0.49)	$\Sigma_{\alpha,22}$	0.07	0.07 (0.03,0.15)
$\mu_{\alpha_b(3)}$	-0.02	0.15 (-0.02,0.33)	$\Sigma_{\alpha,33}$	0.13	0.14 (0.07,0.27)
μ_{α_A}	-0.40	-0.26 (-0.41,-0.10)	$\Sigma_{\alpha,44}$	0.09	0.09 (0.04,0.19)
$\mu_{\alpha_v(1)}$	0.30	0.46 (0.23,0.67)	$\Sigma_{\alpha,55}$	0.22	0.21 (0.10,0.42)
$\mu_{\alpha_v(2)}$	1.12	1.09 (0.99,1.19)	$\Sigma_{\alpha,66}$	0.03	0.04 (0.02,0.08)
μ_{α_τ}	-1.74	-1.84 (-2.01,-1.71)	$\Sigma_{\alpha,77}$	0.09	0.07 (0.03,0.16)

Table 2: Posterior Means with 95% probability intervals of the LBA parameters (the off diagonal elements of Σ_α) estimated using the PMwG method in the simulation study.

Param	True	Est	Param	True	Est	Param	True	Est
$\Sigma_{\alpha,12}$	0.06	0.07 (0.03,0.14)	$\Sigma_{\alpha,24}$	0.06	0.07 (0.03,0.15)	$\Sigma_{\alpha,37}$	-0.09	-0.09 (-0.18,-0.03)
$\Sigma_{\alpha,13}$	0.08	0.09 (0.04,0.19)	$\Sigma_{\alpha,25}$	0.08	0.06 (0.01,0.16)	$\Sigma_{\alpha,45}$	0.04	0.09 (0.02,0.20)
$\Sigma_{\alpha,14}$	0.06	0.07 (0.03,0.15)	$\Sigma_{\alpha,26}$	0.01	0.01 (-0.01,0.05)	$\Sigma_{\alpha,46}$	-0.00	0.00 (-0.03,0.04)
$\Sigma_{\alpha,15}$	0.07	0.06 (0.01,0.16)	$\Sigma_{\alpha,27}$	-0.06	-0.06 (-0.14,-0.03)	$\Sigma_{\alpha,47}$	-0.05	-0.07 (-0.14,-0.03)
$\Sigma_{\alpha,16}$	0.00	0.01 (-0.01,0.05)	$\Sigma_{\alpha,34}$	0.08	0.10 (0.04,0.20)	$\Sigma_{\alpha,55}$	0.01	-0.02 (-0.07,0.02)
$\Sigma_{\alpha,17}$	-0.06	-0.06 (-0.14,-0.02)	$\Sigma_{\alpha,35}$	0.11	0.09 (0.01,0.21)	$\Sigma_{\alpha,56}$	-0.10	-0.08 (-0.18,-0.02)
$\Sigma_{\alpha,23}$	0.09	0.10 (0.04,0.20)	$\Sigma_{\alpha,36}$	0.01	0.02 (-0.01,0.07)	$\Sigma_{\alpha,67}$	-0.00	-0.00 (-0.03,0.02)

Figure 3: Kernel density estimates of some of the individual level random effect parameters α_A and $\alpha_{v_{(j)}^2}$ estimated using the PMwG method. The vertical lines denote the true values.

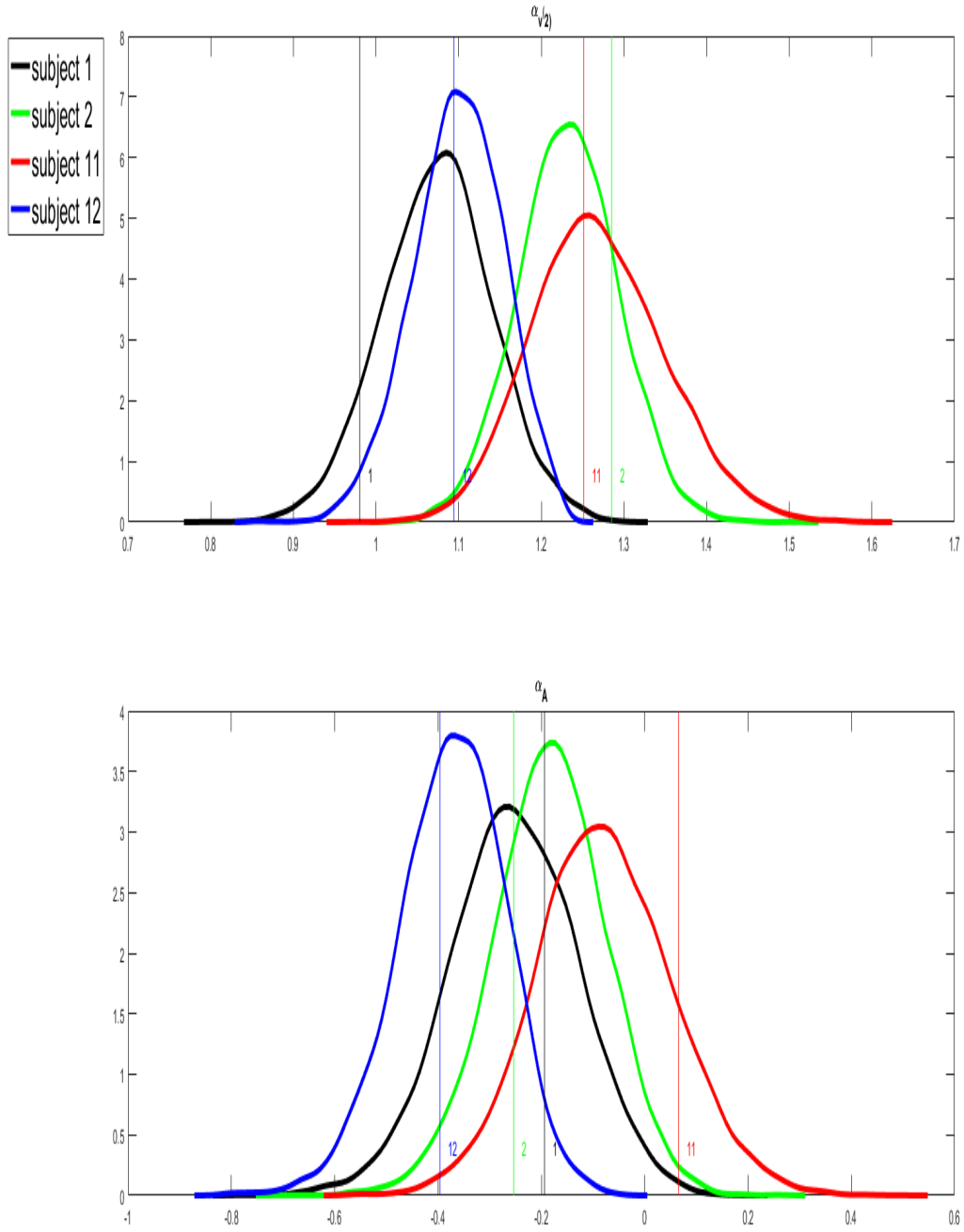


Figure 4: Kernel density estimates of the marginal posterior density over $\mu_{\alpha_b(1)}$, $\mu_{\alpha_b(2)}$, and $\mu_{\alpha_b(3)}$, using the PMwG samples. The vertical lines denote the true values

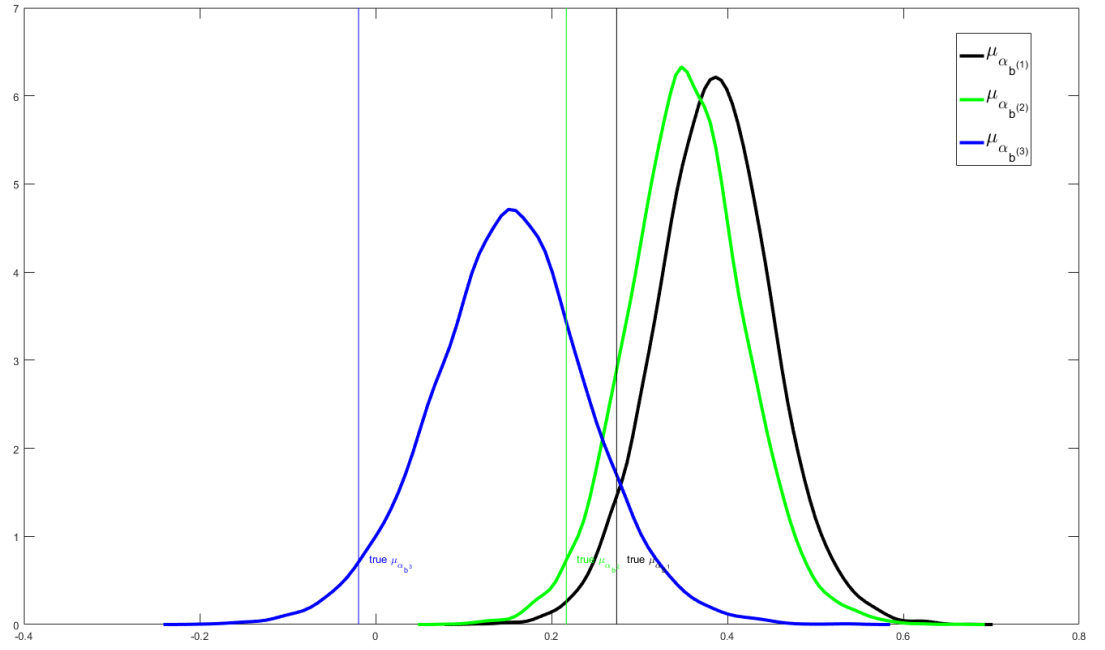
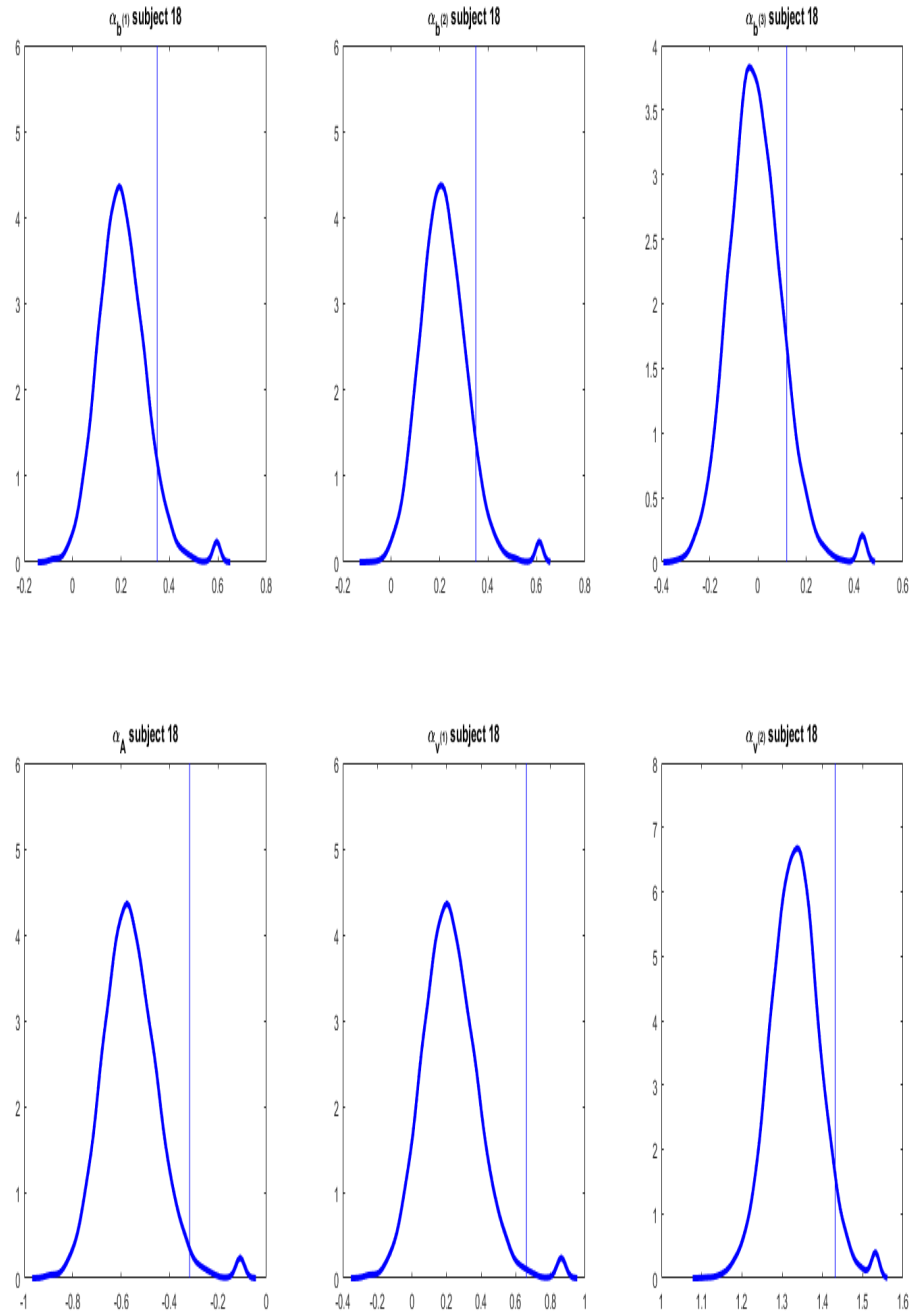


Figure 5: Kernel density estimates of some of the individual level random effect parameters for subject 18 using samples from the PMwG method. The vertical lines denote the true values.



Comparing the PMwG sampler to some existing estimation methods

The hierarchical LBA model is most often estimated using DE-MCMC as in Turner et al. (2013). This section compares the performance of the PMwG sampler to the DE-MCMC sampler, and to a sampler implemented using STAN.

We use DE-MCMC to estimate a simplified hierarchical LBA model which assumes an independent normal distribution for each individual random effects

$$\begin{aligned}\alpha_{b_j^{(z)}} &\sim N\left(\mu_{\alpha_{b_j^{(z)}}}, \sigma_{\alpha_{b_j^{(z)}}}^2\right), \\ \alpha_A &\sim N\left(\mu_{\alpha_A}, \sigma_{\alpha_A}^2\right), \\ \alpha_{v_j^{(z)}} &\sim N\left(\mu_{v_j^{(z)}}, \sigma_{v_j^{(z)}}^2\right), \\ \alpha_\tau &\sim N\left(\mu_\tau, \sigma_\tau^2\right).\end{aligned}$$

We take these following prior densities on the individual random effects, $p\left(\mu_{\alpha_{b_j^{(z)}}}\right) \sim N(0, 3^2)$ for $z = 1, \dots, 3$, $p\left(\mu_{\alpha_A}\right) \sim N(1, 3^2)$, $p\left(\mu_{\alpha_{v_j^{(1)}}}\right) = p\left(\mu_{\alpha_{v_j^{(2)}}}\right) \sim N(1, 3^2)$, $p\left(\mu_\tau\right) \sim N(-2, 1)$, and we take $N(0, 3^2)$ for the log-transformation of the standard deviation parameters for each individual random effects.

Note that we only consider the diagonal elements of Σ_α in this simplified LBA model. To go further than this, and consider the off-diagonal elements, would require the extension of the DE-MCMC approach to estimate the full covariance matrices Σ_α . This is beyond the scope of the present paper. A potential problem for such an extension of DE-MCMC is the greatly increased dimension of the parameter space. The number of parameters to be estimated in the covariance matrix grows with the square of the number of random effects, which could be problematic for DE-MCMC in larger problems. On the other hand, our PMwG scales better than DE-MCMC when the dimension of individual random effects gets bigger because we use a Gibbs step for sampling the LBA parameters $(\mu_\alpha, \Sigma_\alpha)$, rather than the Metropolis-Hastings step used in DE-MCMC.

For the DE-MCMC method, we used 30 chains and each ran for 7660 samples. We discarded the first 1000 iterations from each chain, and kept every 20 draws afterwards. In total, we obtain 9990 samples. The left and right figure of the Figure 6 show the trace plots of some LBA parameters estimated using PMwG and DE-MCMC methods, respectively. It is clear to see that even with 30 parallel chains and kept every 20 for each chain after burn in, the DE-MCMC samples do not mix well. On the other hand, PMwG samples are substantially better than those obtained from DE-MCMC sampler, even without thinning. The left and right figure of the Figure 7

show the trace plots of some of the individual random effects estimated using PMwG and DE-MCMC methods, respectively. Similar conclusions can be drawn from the trace plot of random effects as for the trace plot of the LBA parameters.

As discussed in previous section that the wall-clock computation time to run PMwG samplers was around 35.56 minutes, including the burn in and the initial adaptation stages. This is faster than the equivalent computation using DE-MCMC, which takes 180 minutes using an R implementation.

Yet another approach to estimating the LBA model was describe by Annis et al. (2017). They show how to estimate the simplified hierarchical LBA model as in Turner et al. (2013), assuming an independent truncated normal distribution for the individual random effects, using the STAN programming language. STAN uses the No-U-Turn (NUTS) Hamiltonian Monte Carlo sampler of Hoffman and Gelman (2014). They mention that the hierarchical LBA implementations with STAN can be slow to compute: for 20 subjects, each with 100 data, computation time was approximately 3-6 hours. This is much slower than the PMwG sampler here (and slower than DE-MCMC).

Figure 6: Left Panels: Trace Plots of some of the LBA individual random effects estimated using PMwG method for LBA model defined in Section 2, Right Panels: Trace Plots of some of the LBA individual random effects estimated using DE-MCMC for simplified LBA model.

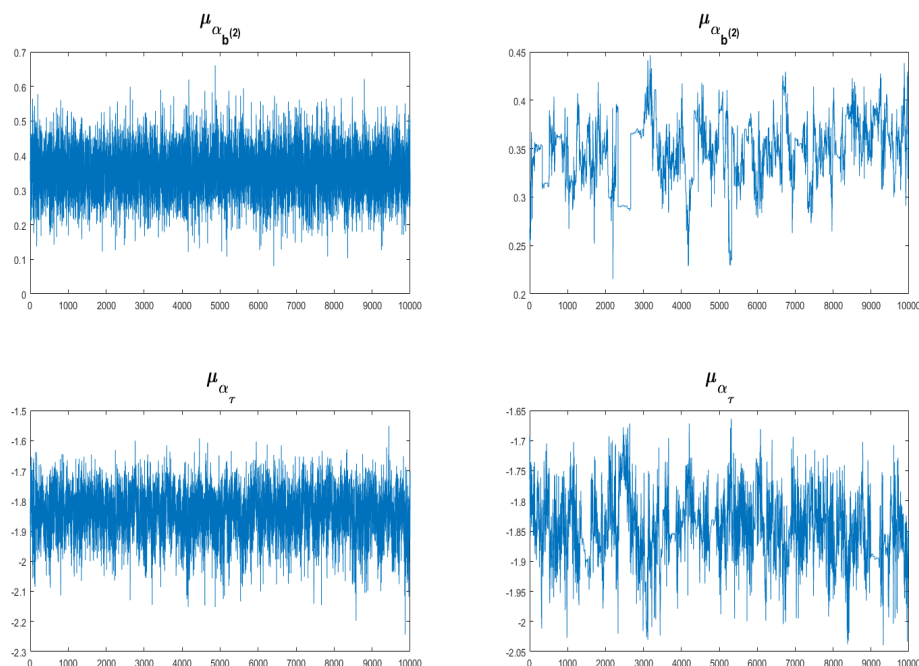
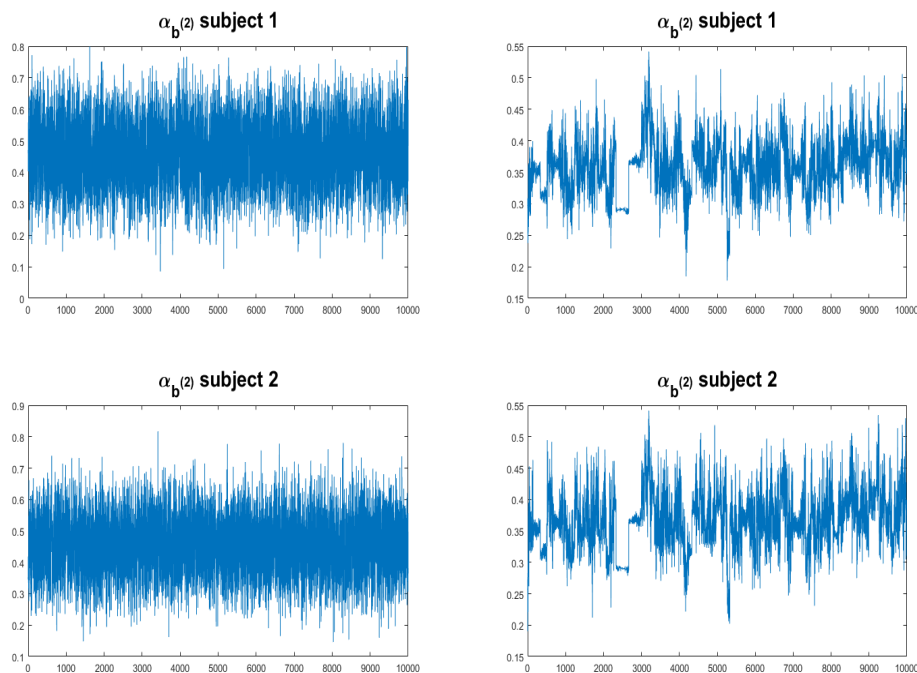


Figure 7: Left Panels: Trace Plots of some of the LBA individual random effects estimated using PMwG method for LBA model defined in Section 2, Right Panels: Trace Plots of some of the LBA individual random effects estimated using DE-MCMC for simplified LBA model.



4.2 Application to Real Data

We applied the PMwG and AISIL-RE methods to the behavioural data first presented by Forstmann et al. (2008), which were introduced in Section 2.1. The PMwG and AISIL-RE methods were run with the same settings as in Section 4.1.

The wall-clock computation time to run the PMwG and the AISIL-RE methods were around 48.37 and 138.74 minutes, respectively, using a Matlab implementation of the algorithm and 28 CPU-cores of a high performance computer cluster.

Table 3 and 4 and Figure 11 in Appendix B show the inefficiency factors for the group-level parameters and individual random effects in the LBA model for the real dataset. Again, all the inefficiency factors (IACT) of the parameters are small, which indicates that chains mixed well and that the performance of the sampler did not deteriorate markedly when moving from simulated data to real data. Table 3 and 4 also show that the estimates of the parameters from PMwG and AISIL-RE methods are very close to each other, which provides a reassuring check. Figures 8 and 9 show the kernel density estimates of marginal posterior densities of some of the LBA individual random effects and parameters based on PMwG and AISIL-

RE samples. These figures show that the AISIL-RE estimates are very close to the PMwG estimates for all parameters.

Tables 5 and 6 summarize the estimates of the posteriors of the parameters of the LBA model and show that there is only a slight difference in the estimates of the mean of the threshold parameters (defined in Eq. (7)) $\{\boldsymbol{\mu}_{LN,\alpha_{b(1)}}, \boldsymbol{\mu}_{LN,\alpha_{b(2)}}, \boldsymbol{\mu}_{LN,\alpha_{b(3)}}\}$ between all three conditions (accuracy, neutral, and speed). The estimate of the maximum of the start point distribution $\boldsymbol{\mu}_{LN,\alpha_A}$ is 0.70, which is smaller than the estimates of the mean of the threshold parameters in all three conditions $(\boldsymbol{\mu}_{LN,\alpha_{b(1)}}, \boldsymbol{\mu}_{LN,\alpha_{b(2)}}, \boldsymbol{\mu}_{LN,\alpha_{b(3)}})$. The estimates of the mean of the drift rate for the incorrect $(\boldsymbol{\mu}_{LN,\alpha_{v(1)}})$ and the correct accumulators $(\boldsymbol{\mu}_{LN,\alpha_{v(2)}})$ are 1.52 and 3.14, respectively. The estimates of mean of non-decision time parameter is 0.18 seconds.

We obtained 168 posterior estimates in total for this model - 133 individual random effects posteriors and 35 group level parameter posteriors. The model setup in Section 2 allows us to obtain the estimates of correlation matrix between individual level parameters:

$$\Gamma = \text{diag}(\boldsymbol{\Sigma}_{LN,\alpha})^{-\frac{1}{2}} \boldsymbol{\Sigma}_{LN,\alpha} \text{diag}(\boldsymbol{\Sigma}_{LN,\alpha})^{-\frac{1}{2}}. \quad (18)$$

Table 6 shows that the threshold parameters for all three conditions are highly correlated, for example $\Gamma(b^{(1)}, b^{(2)}) = 0.96$, $\Gamma(b^{(1)}, b^{(3)}) = 0.87$, and $\Gamma(b^{(2)}, b^{(3)}) = 0.93$. We also found that the maximum of the start point distribution A is highly correlated with the threshold parameters $\Gamma(b^{(1)}, A) = 0.80$, $\Gamma(b^{(2)}, A) = 0.76$, and $\Gamma(b^{(3)}, A) = 0.70$. Interestingly, the non-decision time parameters at the individual subject level are negatively correlated with all other individual level parameters – presumably because of trade-offs between explaining the same RT as either composed of more or less decision time vs. non-decision time. The mean drift rate for the correct accumulators is not highly correlated with all the other individual level parameters.

As mentioned above, there were relatively small differences in the estimates of the mean of the threshold parameters $(\boldsymbol{\mu}_{LN,\alpha_{b(1)}}, \boldsymbol{\mu}_{LN,\alpha_{b(2)}}, \boldsymbol{\mu}_{LN,\alpha_{b(3)}})$ between conditions (accuracy, neutral, and speed). To test this effect, we estimated a restricted model with two threshold parameters by combining the accuracy and neutral conditions, and also a more restricted model with a single and shared threshold parameters for all conditions. We used the AISIL-RE method, with the same specifications as above, to estimate the marginal likelihood for each model. Tables 8 and 9 in Appendix B show the estimates of the parameters of the restricted model that allowed two threshold parameters. We can see that the estimates of $\boldsymbol{\mu}_{LN,\alpha_{b(2)}}, \boldsymbol{\mu}_{LN,\alpha_A}, \boldsymbol{\mu}_{LN,\alpha_{v(1)}}, \boldsymbol{\mu}_{LN,\alpha_{v(2)}},$ and $\boldsymbol{\mu}_{LN,\alpha_\tau}$ in this model are similar to the corresponding unrestricted

model with three threshold parameters. The estimate of $\mu_{LN,\alpha_{b(1)}}$ in the restricted model lies between the estimates of $\mu_{LN,\alpha_{b(1)}}$ and $\mu_{LN,\alpha_{b(2)}}$ of the unrestricted model. The correlation between individual random effects for both the unrestricted and the restricted model with two threshold parameters are also similar.

Tables 10 and 11 in Appendix B show the estimates of the parameters of the more restricted model, with only one threshold parameter. The estimates of μ_{LN,α_b} from this model is larger than all three threshold parameters from the unrestricted LBA model $(\mu_{LN,\alpha_{b(1)}}, \mu_{LN,\alpha_{b(2)}}, \mu_{LN,\alpha_{b(3)}})$. The estimates of the mean of the start point distribution of the restricted model is also larger than the unrestricted model. All other parameters such as $\mu_{LN,\alpha_{v(1)}}$, $\mu_{LN,\alpha_{v(2)}}$, and μ_{LN,α_τ} are quite similar. The correlation between b and A , $\Gamma(b, A) = 0.28$ in the restricted model is substantially smaller than the correlations between the threshold parameters and the starting point in the unrestricted model.

We compared the estimate of the log of the marginal likelihood between the unrestricted model, the restricted model with two threshold parameters, and the more restricted model with one threshold parameter. The estimated log marginal likelihoods (with standard errors) for the unrestricted model, the restricted model with two threshold parameters, and the restricted model with one threshold parameter were: 7448.39 (2.40), 7351.32 (1.96) and 5199.64 (1.29), respectively. The differences between the likelihoods are much larger than the standard errors of the sampling, and also large relative to the scales usually used to judge statistical reliability (e.g. the corresponding Bayes factors for the model comparisons are all much larger than 10^6). These results favour the unrestricted model for these data, which also supports the analyses of Forstmann et al. (2008).

Table 3: Posterior means (with posterior standard deviation in brackets), and Inefficiency Factors (IACT) of the LBA parameters (all the μ_α and the diagonal elements of Σ_α) of the full model estimated using PMwG and AISIL-RE. The order of random effect parameters in the covariance matrix Σ_α is $\alpha_{b(1)}$, $\alpha_{b(2)}$, $\alpha_{b(3)}$, α_A , $\alpha_{v(1)}$, $\alpha_{v(2)}$, and α_τ .

Param.	Est	IACT	Est	Param.	Est	IACT	Est
	PMwG	PMwG	AISIL-RE		PMwG	PMwG	AISIL-RE
$\mu_{\alpha_{b(1)}}$	0.27 (0.06)	1.22	0.28 (0.06)	$\Sigma_{\alpha,11}$	0.06 (0.03)	1.68	0.06 (0.03)
$\mu_{\alpha_{b(2)}}$	0.22 (0.06)	1.17	0.22 (0.06)	$\Sigma_{\alpha,22}$	0.07 (0.03)	1.62	0.07 (0.03)
$\mu_{\alpha_{b(3)}}$	-0.02 (0.08)	1.10	-0.01 (0.09)	$\Sigma_{\alpha,33}$	0.13 (0.05)	1.49	0.13 (0.05)
μ_{α_A}	-0.40 (0.07)	1.49	-0.40 (0.07)	$\Sigma_{\alpha,44}$	0.09 (0.04)	2.61	0.09 (0.04)
$\mu_{\alpha_{v(1)}}$	0.30 (0.11)	1.26	0.31 (0.11)	$\Sigma_{\alpha,55}$	0.22 (0.09)	2.00	0.22 (0.08)
$\mu_{\alpha_{v(2)}}$	1.12 (0.04)	1.28	1.13 (0.04)	$\Sigma_{\alpha,66}$	0.03 (0.02)	2.53	0.03 (0.02)
μ_{α_τ}	-1.74 (0.07)	2.16	-1.75 (0.07)	$\Sigma_{\alpha,77}$	0.09 (0.04)	5.70	0.09 (0.04)

Table 4: Posterior Means (with posterior standard deviations in brackets), and inefficiency factors (IACT) of the LBA parameters (the off diagonal elements of Σ_α) of the full model estimated using PMwG and AISIL-RE. The order of random effect parameters in the covariance matrix Σ_α is $\alpha_{b(1)}$, $\alpha_{b(2)}$, $\alpha_{b(3)}$, α_A , $\alpha_{v(1)}$, $\alpha_{v(2)}$, and α_τ .

Param.	Est	IACT	Est	Param.	Est	IACT	Est	Param.	Est	IACT	Est
	PMwG	PMwG	AISIL		PMwG	PMwG	AISIL		PMwG	PMwG	AISIL
$\Sigma_{\alpha,12}$	0.06 (0.03)	1.66	0.07 (0.03)	$\Sigma_{\alpha,24}$	0.06 (0.03)	1.56	0.06 (0.03)	$\Sigma_{\alpha,37}$	-0.09 (0.04)	2.89	-0.09 (0.04)
$\Sigma_{\alpha,13}$	0.08 (0.03)	1.61	0.08 (0.04)	$\Sigma_{\alpha,25}$	0.08 (0.04)	1.72	0.08 (0.04)	$\Sigma_{\alpha,45}$	0.04 (0.04)	1.70	0.04 (0.04)
$\Sigma_{\alpha,14}$	0.06 (0.03)	1.63	0.06 (0.03)	$\Sigma_{\alpha,26}$	0.01 (0.01)	1.71	0.01 (0.01)	$\Sigma_{\alpha,46}$	-0.00 (0.01)	1.60	-0.00 (0.02)
$\Sigma_{\alpha,15}$	0.06 (0.04)	1.70	0.07 (0.04)	$\Sigma_{\alpha,27}$	-0.06 (0.03)	3.05	-0.06 (0.03)	$\Sigma_{\alpha,47}$	-0.05 (0.03)	2.00	-0.05 (0.03)
$\Sigma_{\alpha,16}$	0.00 (0.01)	1.61	0.00 (0.01)	$\Sigma_{\alpha,34}$	0.08 (0.04)	1.53	0.08 (0.04)	$\Sigma_{\alpha,56}$	0.01 (0.02)	1.58	0.01 (0.02)
$\Sigma_{\alpha,17}$	-0.05 (0.03)	2.67	-0.05 (0.03)	$\Sigma_{\alpha,35}$	0.11 (0.05)	1.59	0.11 (0.05)	$\Sigma_{\alpha,57}$	-0.09 (0.05)	2.82	-0.10 (0.05)
$\Sigma_{\alpha,23}$	0.09 (0.04)	1.56	0.09 (0.04)	$\Sigma_{\alpha,36}$	0.01 (0.02)	1.56	0.01 (0.02)	$\Sigma_{\alpha,67}$	-0.00 (0.01)	1.57	-0.00 (0.01)

Figure 8: Kernel density estimates of some of the LBA parameters of the full model.

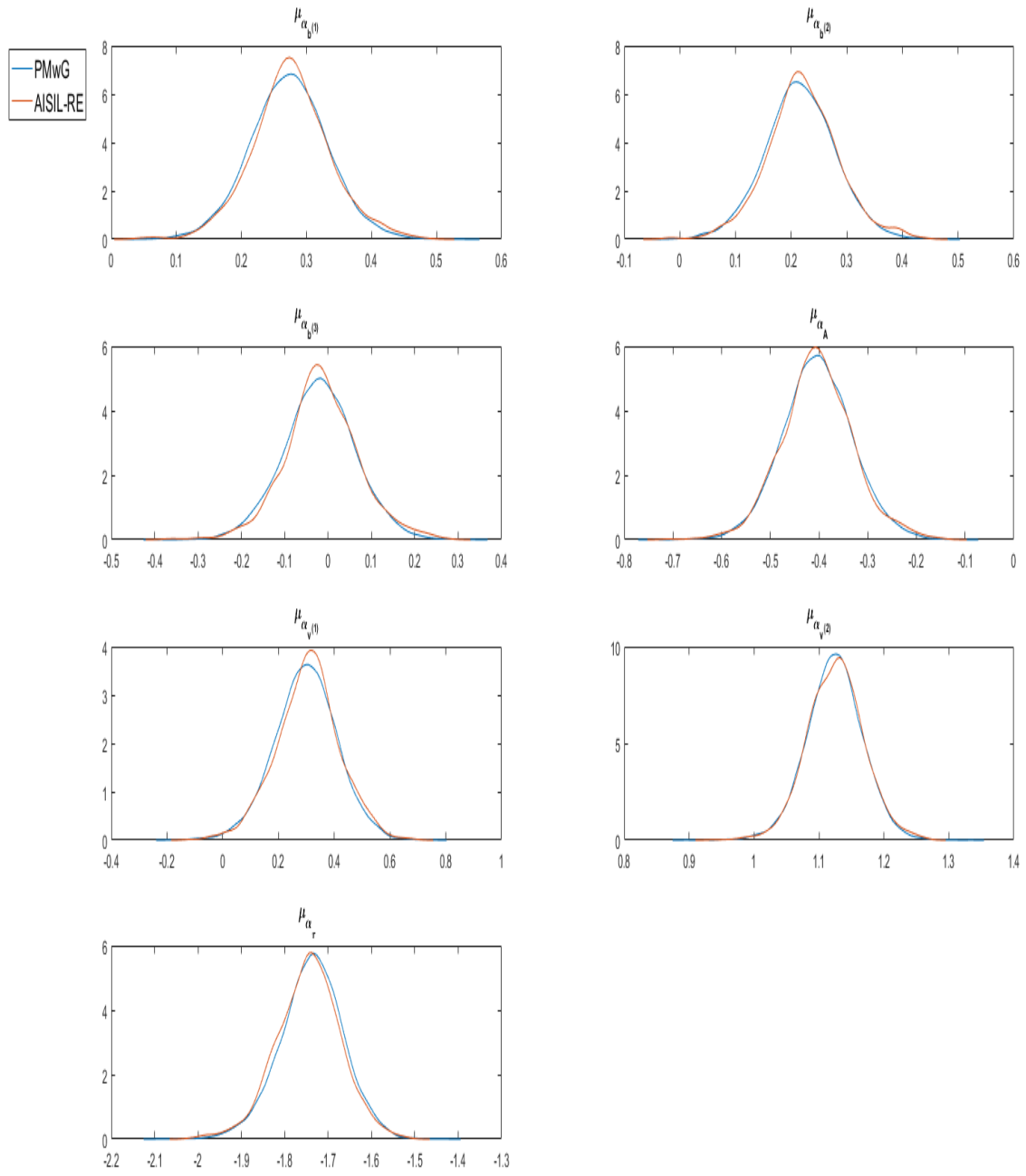


Figure 9: Kernel density estimates some of the individual level random effects parameters of the full model

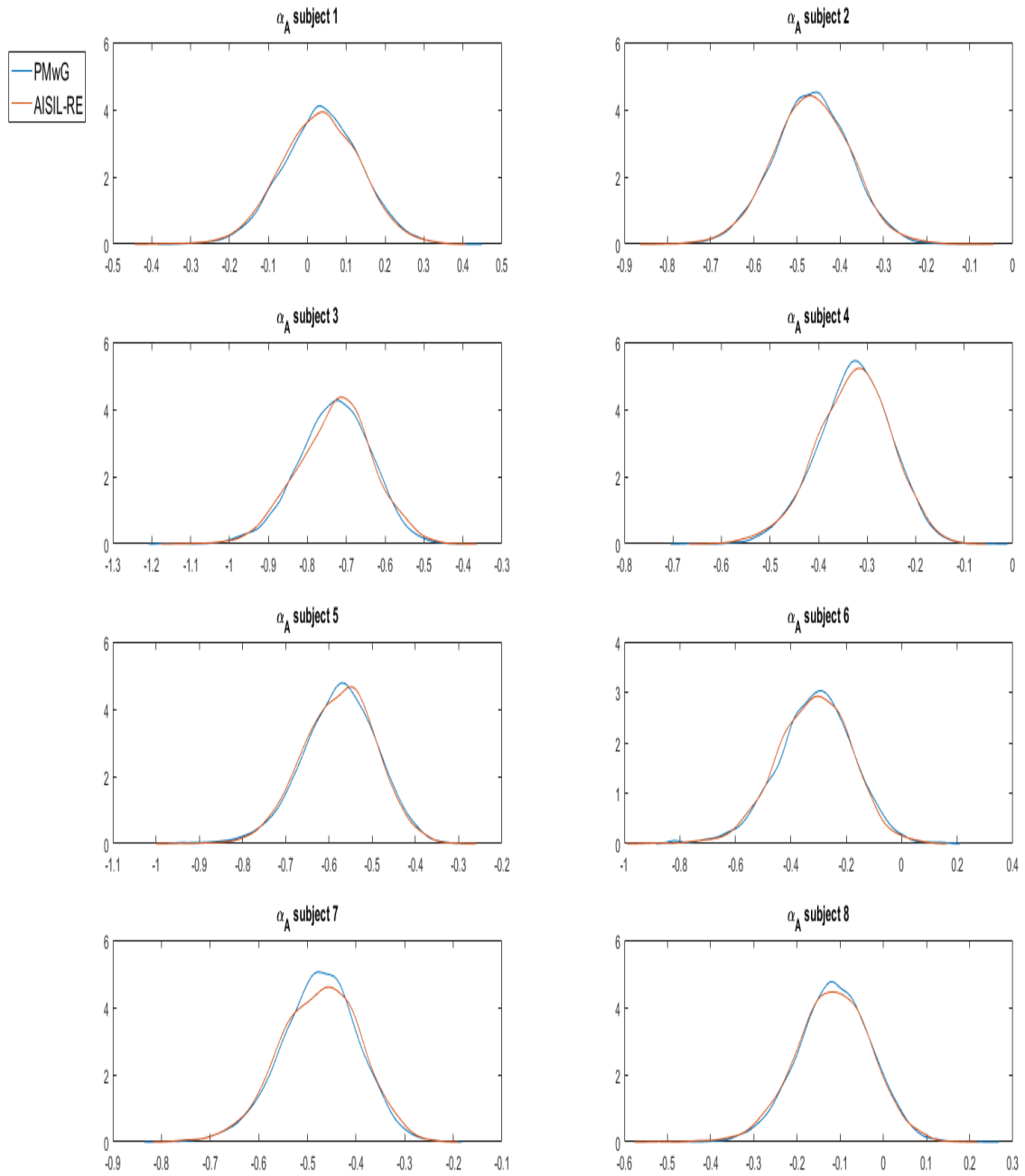


Table 5: Posterior means (with posterior standard deviation in brackets) of the LBA parameters of the full/unrestricted model with three threshold parameters obtained using AISIL-RE method. The order of random effect parameters in the covariance matrix Σ_α is $b^{(1)}$, $b^{(2)}$, $b^{(3)}$, A , $v^{(1)}$, $v^{(2)}$, and τ , respectively.

Param.	Est.	Param.	Est.	Param.	Est.	Param.	Est.	Param.	Est.
$\mu_{LN,\alpha_{b^{(1)}}}$	1.36 (0.08)	$\Sigma_{LN,\alpha,11}$	0.13 (0.06)	$\Sigma_{LN,\alpha,22}$	0.13 (0.06)	$\Sigma_{LN,\alpha,34}$	0.06 (0.04)	$\Sigma_{LN,\alpha,47}$	-0.01 (0.00)
$\mu_{LN,\alpha_{b^{(2)}}}$	1.30 (0.09)	$\Sigma_{LN,\alpha,12}$	0.12 (0.06)	$\Sigma_{LN,\alpha,23}$	0.13 (0.07)	$\Sigma_{LN,\alpha,35}$	0.19 (0.12)	$\Sigma_{LN,\alpha,55}$	0.60 (0.37)
$\mu_{LN,\alpha_{b^{(3)}}}$	1.06 (0.09)	$\Sigma_{LN,\alpha,13}$	0.12 (0.07)	$\Sigma_{LN,\alpha,24}$	0.06 (0.03)	$\Sigma_{LN,\alpha,36}$	0.04 (0.07)	$\Sigma_{LN,\alpha,56}$	0.07 (0.12)
μ_{LN,α_A}	0.70 (0.05)	$\Sigma_{LN,\alpha,14}$	0.06 (0.03)	$\Sigma_{LN,\alpha,25}$	0.16 (0.10)	$\Sigma_{LN,\alpha,37}$	-0.01 (0.01)	$\Sigma_{LN,\alpha,57}$	-0.02 (0.01)
$\mu_{LN,\alpha_{v^{(1)}}}$	1.52 (0.18)	$\Sigma_{LN,\alpha,15}$	0.13 (0.09)	$\Sigma_{LN,\alpha,26}$	0.02 (0.06)	$\Sigma_{LN,\alpha,44}$	0.05 (0.03)	$\Sigma_{LN,\alpha,66}$	0.34 (0.17)
$\mu_{LN,\alpha_{v^{(2)}}}$	3.14 (0.14)	$\Sigma_{LN,\alpha,16}$	0.01 (0.05)	$\Sigma_{LN,\alpha,27}$	-0.01 (0.01)	$\Sigma_{LN,\alpha,45}$	0.05 (0.05)	$\Sigma_{LN,\alpha,67}$	-0.00 (0.01)
μ_{LN,α_τ}	0.18 (0.01)	$\Sigma_{LN,\alpha,17}$	-0.01 (0.01)	$\Sigma_{LN,\alpha,33}$	0.16 (0.09)	$\Sigma_{LN,\alpha,46}$	-0.00 (0.04)	$\Sigma_{LN,\alpha,77}$	0.003 (0.002)

Table 6: Posterior means (with posterior standard deviation in brackets) of the correlation parameters of the LBA parameters of the full/unrestricted model with three threshold parameters obtained using AISIL-RE method.

Param.	Est.	Param.	Est.	Param.	Est.
$\Gamma_{(b^{(1)},b^{(2)})}$	0.96 (0.02)	$\Gamma_{(b^{(2)},A)}$	0.76 (0.12)	$\Gamma_{(b^{(3)},\tau)}$	-0.70 (0.06)
$\Gamma_{(b^{(1)},b^{(3)})}$	0.87 (0.05)	$\Gamma_{(b^{(2)},v^{(1)})}$	0.57 (0.14)	$\Gamma_{(A,v^{(1)})}$	0.27 (0.20)
$\Gamma_{(b^{(1)},A)}$	0.80 (0.10)	$\Gamma_{(b^{(2)},v^{(2)})}$	0.09 (0.23)	$\Gamma_{(A,v^{(2)})}$	-0.03 (0.23)
$\Gamma_{(b^{(1)},v^{(1)})}$	0.49 (0.16)	$\Gamma_{(b^{(2)},\tau)}$	-0.69 (0.07)	$\Gamma_{(A,\tau)}$	-0.46 (0.16)
$\Gamma_{(b^{(1)},v^{(2)})}$	0.03 (0.23)	$\Gamma_{(b^{(3)},A)}$	0.70 (0.14)	$\Gamma_{(v^{(1)},v^{(2)})}$	0.16 (0.22)
$\Gamma_{(b^{(1)},\tau)}$	-0.63 (0.09)	$\Gamma_{(b^{(3)},v^{(1)})}$	0.62 (0.14)	$\Gamma_{(v^{(1)},\tau)}$	-0.55 (0.09)
$\Gamma_{(b^{(2)},b^{(3)})}$	0.93 (0.03)	$\Gamma_{(b^{(3)},v^{(2)})}$	0.14 (0.23)	$\Gamma_{(v^{(2)},\tau)}$	-0.03 (0.22)

5 Conclusions

Based on recent advances in particle Markov chain Monte-Carlo, we have developed two new estimation approaches for the Linear Ballistic Accumulator model of Brown and Heathcote (2008); the Particle Metropolis within Gibbs and Annealed importance sampling algorithms. We showed that the PMwG and AISIL-RE methods perform well for both real and simulated datasets. The proposed PMwG and AISIL-RE methods can be considered as an alternative to the existing approach that is based on MCMC with proposals generated by differential evolution (Turner et al., 2013). These new methods provide important advantages. The PMwG method has

greatly reduced autocorrelation (i.e. redundancy) in the Markov chains compared with the existing DE-MCMC approach. Both methods are also very well-suited for parallelisation in high-performance computing environments. The current approach of DE-MCMC implies frequent dependence between the multiple chains, which limits the efficiency of the sampler when parallelised. This limitation is greatly reduced in the AISIL-RE methods.

Another important advance in the methods we have developed is to explicitly model the covariance of the random effects. Like all plausible cognitive models, there are substantial correlations between the parameters of the LBA model for individuals: subjects with a large decision threshold also tend to have a large startup point, and so forth. In previous applications of the model, these correlations were not modelled explicitly, because the group-level distributions were modelled as if independent. Even when making this *a priori* assumption of independence, the resulting posterior samples always exhibited strong correlations between parameters. Explicitly modelling these correlations, as we have done, improves the model’s fit to the data, provides better estimates of the parameters and their variances, and improves computational efficiency.

The advantages of the new methods we have proposed here also allows exploration of important psychological questions which have hitherto been neglected, due to statistical intractability. For example, it is well known that there can be substantial sequential effects in decision-making data: both response choices and response times tend to be positively auto-correlated. All applications of the LBA model – and indeed, almost all decision-making models – have ignored these sequential effects, attributing their results to standard error terms. Both our approaches extend in tractable ways to include explicit accounts of autocorrelation, and other interesting sequential effects, such as evolution in parameters due to fatigue or learning. We are investigating these models in ongoing work.

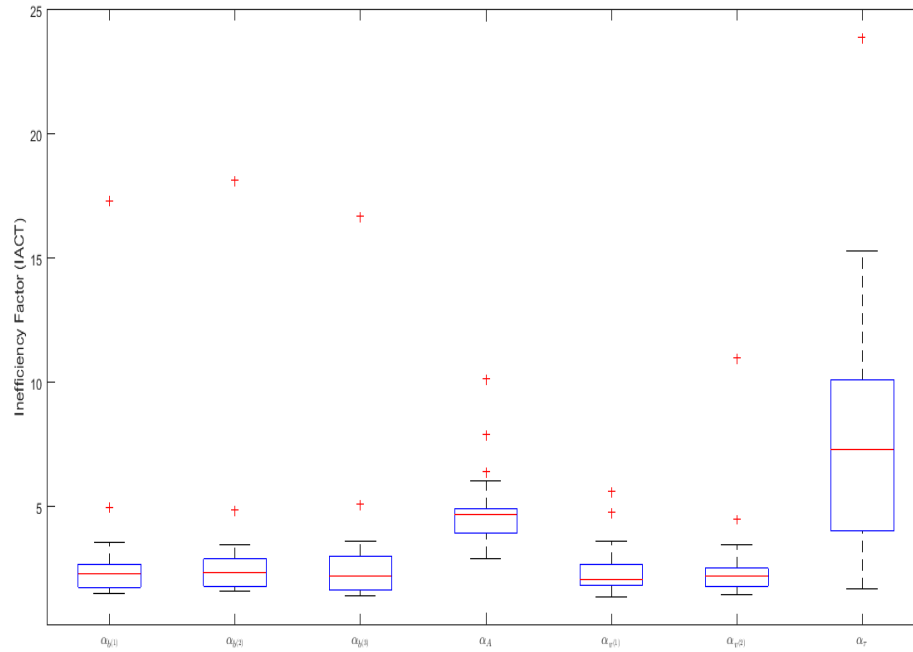
To aid researchers in adopting the methods we have proposed, we also provide some of the scripts used to implement the analyses reported above. The scripts are written in Matlab and are available upon request from the authors. They implement both the PMwG and AISIL-RE methods as applied to the simulated and real data from Forstmann et al. (2008).

A Additional Results for simulated data

Table 7: Inefficiency Factors of the LBA Parameters defined in Section 2.1 estimated using PMwG method

Param.	IACT	Param.	IACT	Param.	IACT	Param.	IACT	Param.	IACT
$\mu_{\alpha_b(1)}$	1.59	$\Sigma_{\alpha,11}$	2.33	$\Sigma_{\alpha,22}$	2.38	$\Sigma_{\alpha,34}$	2.85	$\Sigma_{\alpha,47}$	2.71
$\mu_{\alpha_b(2)}$	1.67	$\Sigma_{\alpha,12}$	2.38	$\Sigma_{\alpha,23}$	2.21	$\Sigma_{\alpha,35}$	1.89	$\Sigma_{\alpha,55}$	2.19
$\mu_{\alpha_b(3)}$	1.27	$\Sigma_{\alpha,13}$	2.23	$\Sigma_{\alpha,24}$	2.97	$\Sigma_{\alpha,36}$	2.45	$\Sigma_{\alpha,56}$	1.97
μ_{α_A}	4.03	$\Sigma_{\alpha,14}$	2.80	$\Sigma_{\alpha,25}$	2.29	$\Sigma_{\alpha,37}$	4.77	$\Sigma_{\alpha,57}$	3.12
$\mu_{\alpha_v(1)}$	1.34	$\Sigma_{\alpha,15}$	1.85	$\Sigma_{\alpha,26}$	2.66	$\Sigma_{\alpha,44}$	3.76	$\Sigma_{\alpha,66}$	3.02
$\mu_{\alpha_v(2)}$	1.80	$\Sigma_{\alpha,16}$	2.64	$\Sigma_{\alpha,27}$	5.07	$\Sigma_{\alpha,45}$	2.28	$\Sigma_{\alpha,67}$	2.87
μ_{α_τ}	9.16	$\Sigma_{\alpha,17}$	5.08	$\Sigma_{\alpha,33}$	1.91	$\Sigma_{\alpha,46}$	2.62	$\Sigma_{\alpha,77}$	10.62

Figure 10: The Inefficiency Factor of Individual Level Random Effects Parameters. Each boxplot shows the distribution of IACT across participants, for one of the model parameters, estimated using PMwG method with specification given in Section 2.1. The outliers correspond to parameters for subject 9.



B Additional Results for real data

Table 8: Posterior means (with posterior standard deviations in brackets) of the LBA parameters of the restricted model with two threshold parameter obtained using AISIL-RE method. The order of random effect parameters in the covariance matrix Σ is $b^{(1)}$, $b^{(2)}$, A , $v^{(1)}$, $v^{(2)}$, and τ , respectively.

Param.	Est.	Param.	Est.	Param.	Est.	Param.	Est.	Param.	Est.
$\mu_{LN,\alpha_{b^{(1)}}}$	1.33 (0.09)	$\Sigma_{LN,\alpha,11}$	0.13 (0.07)	$\Sigma_{LN,\alpha,22}$	0.16 (0.10)	$\Sigma_{LN,\alpha,34}$	0.05 (0.06)	$\Sigma_{LN,\alpha,55}$	0.33 (0.17)
$\mu_{LN,\alpha_{b^{(2)}}}$	1.06 (0.09)	$\Sigma_{LN,\alpha,12}$	0.13 (0.08)	$\Sigma_{LN,\alpha,23}$	0.06 (0.04)	$\Sigma_{LN,\alpha,35}$	-0.00 (0.03)	$\Sigma_{LN,\alpha,56}$	-0.00 (0.01)
μ_{LN,α_A}	0.70 (0.05)	$\Sigma_{LN,\alpha,13}$	0.06 (0.04)	$\Sigma_{LN,\alpha,24}$	0.20 (0.16)	$\Sigma_{LN,\alpha,36}$	-0.01 (0.00)	$\Sigma_{LN,\alpha,66}$	0.003 (0.002)
$\mu_{LN,\alpha_{v^{(1)}}}$	1.53 (0.18)	$\Sigma_{LN,\alpha,14}$	0.16 (0.12)	$\Sigma_{LN,\alpha,25}$	0.04 (0.06)	$\Sigma_{LN,\alpha,44}$	0.61 (0.75)		
$\mu_{LN,\alpha_{v^{(2)}}}$	3.13 (0.14)	$\Sigma_{LN,\alpha,15}$	0.02 (0.06)	$\Sigma_{LN,\alpha,26}$	-0.02 (0.01)	$\Sigma_{LN,\alpha,45}$	0.10 (0.13)		
μ_{LN,α_τ}	0.18 (0.01)	$\Sigma_{LN,\alpha,16}$	-0.01 (0.01)	$\Sigma_{LN,\alpha,33}$	0.05 (0.03)	$\Sigma_{LN,\alpha,46}$	-0.02 (0.01)		

Table 9: Posterior means (with posterior standard deviations in brackets) of the correlation parameters of the LBA parameters of the restricted model with two threshold parameters obtained using AISIL-RE method.

Param.	Est.	Param.	Est.	Param.	Est.
$\Gamma_{(b^{(1)},b^{(2)})}$	0.91 (0.04)	$\Gamma_{(b^{(2)},v^{(1)})}$	0.64 (0.14)	$\Gamma_{(v^{(1)},v^{(2)})}$	0.22 (0.21)
$\Gamma_{(b^{(1)},A)}$	0.81 (0.10)	$\Gamma_{(b^{(2)},v^{(2)})}$	0.17 (0.22)	$\Gamma_{(v^{(1)},\tau)}$	-0.59 (0.12)
$\Gamma_{(b^{(1)},v^{(1)})}$	0.56 (0.16)	$\Gamma_{(b^{(2)},\tau)}$	-0.77 (0.06)	$\Gamma_{(v^{(2)},\tau)}$	-0.06 (0.23)
$\Gamma_{(b^{(1)},v^{(2)})}$	0.10 (0.23)	$\Gamma_{(A,v^{(1)})}$	0.33 (0.21)		
$\Gamma_{(b^{(1)},\tau)}$	-0.74 (0.08)	$\Gamma_{(A,v^{(2)})}$	-0.03 (0.23)		
$\Gamma_{(b^{(2)},A)}$	0.74 (0.12)	$\Gamma_{(A,\tau)}$	-0.57 (0.16)		

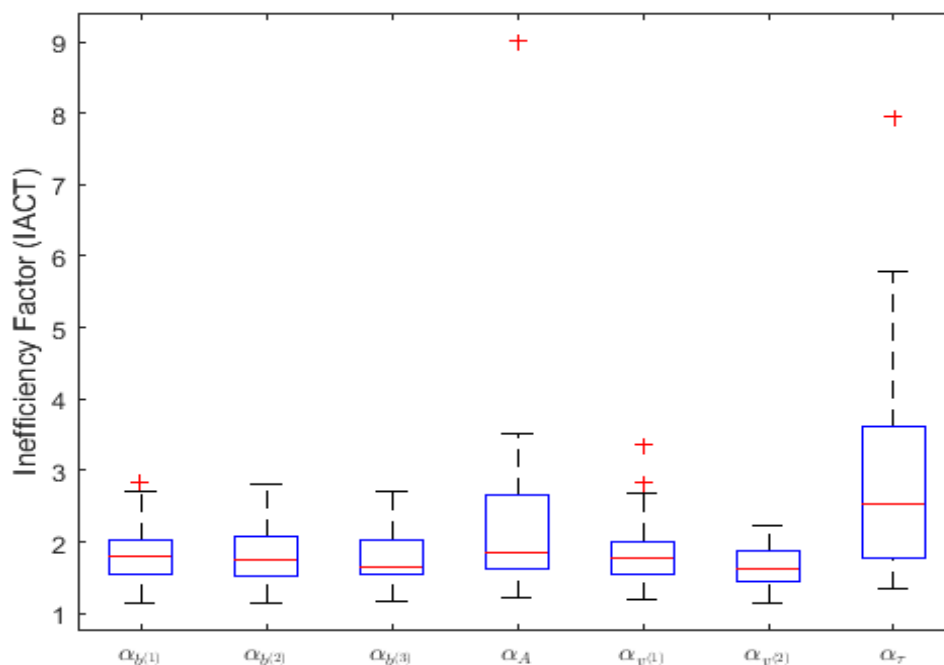
Table 10: Posterior means (with posterior standard deviation in brackets) of the LBA parameters of the restricted model with one threshold parameter obtained using AISIL-RE method. The order of random effect parameters in the covariance matrix Σ is b , A , $v^{(1)}$, $v^{(2)}$, and τ , respectively.

Param.	Est.	Param.	Est.	Param.	Est.	Param.	Est.
μ_{LN,α_b}	1.45 (0.09)	$\Sigma_{LN,\alpha,11}$	0.14 (0.07)	$\Sigma_{LN,\alpha,22}$	0.15 (0.10)	$\Sigma_{LN,\alpha,34}$	0.19 (0.21)
μ_{LN,α_A}	0.96 (0.09)	$\Sigma_{LN,\alpha,12}$	0.04 (0.04)	$\Sigma_{LN,\alpha,23}$	-0.10 (0.10)	$\Sigma_{LN,\alpha,35}$	-0.05 (0.03)
$\mu_{LN,\alpha_{v^{(1)}}}$	1.55 (0.26)	$\Sigma_{LN,\alpha,13}$	0.25 (0.19)	$\Sigma_{LN,\alpha,24}$	-0.09 (0.07)	$\Sigma_{LN,\alpha,44}$	0.40 (0.18)
$\mu_{LN,\alpha_{v^{(2)}}}$	3.24 (0.15)	$\Sigma_{LN,\alpha,14}$	0.04 (0.07)	$\Sigma_{LN,\alpha,25}$	0.01 (0.01)	$\Sigma_{LN,\alpha,45}$	-0.02 (0.02)
μ_{LN,α_τ}	0.17 (0.02)	$\Sigma_{LN,\alpha,15}$	-0.02 (0.02)	$\Sigma_{LN,\alpha,33}$	1.42 (0.97)	$\Sigma_{LN,\alpha,55}$	0.01 (0.01)

Table 11: Posterior means (with posterior standard deviations in brackets) of the correlation parameters of the LBA parameters of the restricted model with one threshold parameter obtained using AISIL method.

Param.	Est.	Param.	Est.
$\Gamma_{(b,A)}$	0.28 (0.21)	$\Gamma_{(A,v^{(2)})}$	-0.37 (0.20)
$\Gamma_{(b,v^{(1)})}$	0.59 (0.14)	$\Gamma_{(A,\tau)}$	0.31 (0.21)
$\Gamma_{(b,v^{(2)})}$	0.15 (0.23)	$\Gamma_{(v^{(1)},v^{(2)})}$	0.27 (0.19)
$\Gamma_{(b,\tau)}$	-0.57 (0.13)	$\Gamma_{(v^{(1)},\tau)}$	-0.60 (0.08)
$\Gamma_{(A,v^{(1)})}$	-0.24 (0.18)	$\Gamma_{(v^{(2)},\tau)}$	-0.35 (0.19)

Figure 11: The Inefficiency Factors of the Individual Level Random Effects Parameters from the full model estimated using the PMwG



C The boundedness of LBA density

Given a choice between two alternatives, the density of the first accumulator reaching the threshold at time t and the second accumulator not reaching the threshold at that time is given by

$$\text{LBA}(1, t|b, A, v, s, \tau) = f_1(t - \tau)(1 - F_2(t - \tau)). \quad (19)$$

To show that $\text{LBA}(1, t|b, A, v, s, \tau)$ is bounded in its argument, it is sufficient to show that $f_1(t - \tau)$ given by Eq. (1) is bounded as $F_2(t - \tau)$ is a cdf and hence always bounded. Now, $f_1(t - \tau)$ will be bounded if $-\frac{v^1}{A}\Phi\left(\frac{b-A-tv^1}{ts}\right)$ and $\frac{v^1}{A}\Phi\left(\frac{b-tv^1}{ts}\right)$ are bounded for all $v^1 > 0$ and the required boundedness follows from the inequality $v\Phi(-v) \leq \phi(v)$ for all $v > 0$.

References

Annis, J., Miller, B. J., and Palmeri, T. J. (2017). Bayesian inference with Stan: a tutorial on adding custom distributions. *Behavioural Research*, 49(863-886).

- Brown, S. and Heathcote, A. (2005). A ballistic model of choice response time. *Psychological Review*, 112:117–128.
- Brown, S. and Heathcote, A. (2008). The simple complete model of choice reaction time: Linear Ballistic accumulation. *Cognitive Psychology*, 57:153–178.
- Chib, S. and Jeliazkov, I. (2001). Marginal likelihood from the Metropolis-Hastings output. *Journal of American Statistical Association*, 96(453):270–281.
- Del Moral, P., Doucet, A., and Jasra, A. (2006). Sequential Monte Carlo samplers. *Journal of the Royal Statistical Society, Series B*, 68:411–436.
- Del Moral, P., Doucet, A., and Jasra, A. (2012). An adaptive Sequential Monte Carlo for approximate Bayesian computation. *Statistics and Computing*, pages 1009–1020.
- Donkin, C. and Brown, S. D. (2018). Response times and decision-making. *Stevens’ Handbook of Experimental Psychology and Cognitive Neuroscience, Methodology*, page 349.
- Donkin, C., Brown, S. D., and Heathcote, A. J. (2009). The over-constraint of response time models: Rethinking the scaling problem. *Psychonomic Bulletin & Review*, 16:1129–1135.
- Duan, J. C. and Fulop, A. (2015). Density-tempered marginalised sequential Monte Carlo samplers. *Journal of Business and Economics Statistics*, 33(2):192–202.
- Evans, N. J. and Brown, S. D. (2018). Bayes factors for the linear ballistic accumulator model of decision-making. *Behavior research methods*, 50(2):589–603.
- Forstmann, B. U., Dutilh, G., Brown, S., Neumann, J., and von Cramon, D. Y. (2008). Striatum and pre-sma facilitate decision making under time pressure. *Proceedings of the National Academy of Sciences*, 105:17538–17542.
- Gronau, Q. F., Sarafoglou, A., Matzke, D., Ly, A., Boehm, U., Marsman, M., Leslie, D. S., Forster, J. J., Wagenmakers, E.-J., and Steingroever, H. (2017). A tutorial on bridge sampling. *Journal of mathematical psychology*, 81:80–97.
- Gunawan, D., Carter, C., Fiebig, D. G., and Kohn, R. (2017). Efficient Bayesian estimation for flexible panel models for multivariate outcomes: impact of life events on mental health and excessive alcohol consumption. *arXiv preprint arXiv:1706.03953v1*.

- Gunawan, D., Kohn, R., Carter, C., and Tran, M. N. (2018). Flexible density tempering approaches for state space models with an application to factor stochastic volatility models. *arXiv:1805.00649v1*.
- Hesterberg, T. (1995). Weighted average importance sampling and defensive mixture distributions. *Technometrics*, 37:185–194.
- Hoffman, M. D. and Gelman, A. (2014). The No-U-Turn sampler: adaptively setting path length in Hamiltonian Monte Carlo. *Journal of Machine Learning Research*, 15:1593–1623.
- Huang, A. and Wand, M. P. (2013). Simple marginally noninformative prior distributions for covariance matrices. *Bayesian Analysis*, 8(2):439–452.
- Kass, R. E. and Raftery, A. E. (1995). Bayes factors. *Journal of American Statistical Association*, 90(430):773–795.
- Neal, R. (2001). Annealed importance sampling. *Statistics and Computing*, 11:125–139.
- Plummer, M., Best, N., Cowles, K., and Vines, K. (2006). CODA: Convergence Diagnosis and Output Analysis of MCMC. *R News*, 6(1):7–11.
- Ratcliff, R. (1978). A theory of memory retrieval. *Psychological Review*, 85:59–108.
- Ratcliff, R. and Rouder, J. N. (1998). Modeling response times for two-choice decisions. *Psychological Science*, 9:347–356.
- Ratcliff, R. and Smith, P. L. (2004). A comparison of sequential sampling models for two-choice reaction time. *Psychological Review*, 111:333–367.
- Ratcliff, R., Smith, P. L., Brown, S. D., and McKoon, G. (2016). Diffusion decision model: current issues and history. *Trends in cognitive sciences*, 20(4):260–281.
- Spiegelhalter, D. J., Best, N. G., Carlin, B. P., and Linde, A. (2014). The deviance information criterion: 12 years on. *Journal of the Royal Statistical Society: Series B (Statistical Methodology)*, 76(3):485–493.
- Terry, A., Marley, A., Barnwal, A., Wagenmakers, E.-J., Heathcote, A., and Brown, S. D. (2015). Generalising the drift rate distribution for linear ballistic accumulators. *Journal of Mathematical Psychology*, 68:49–58.
- Turner, B. M., Sederberg, P. B., Brown, S. D., and Steyvers, M. (2013). A method for efficiently sampling from distributions with correlated dimensions. *Psychological Methods*, 18(3):368–384.

- Usher, M. and McClelland, J. L. (2001). On the time course of perceptual choice: The leaky competing accumulator model. *Psychological Review*, 108:550–592.
- Watanabe, S. (2010). Asymptotic equivalence of bayes cross validation and widely applicable information criterion in singular learning theory. *Journal of Machine Learning Research*, 11(Dec):3571–3594.